

2013

# Design of a Tunable Integrated Roofing Filter for Lte Bands

Nihar Athreyas

*University of Massachusetts Amherst*

Follow this and additional works at: <https://scholarworks.umass.edu/theses>



Part of the [Electrical and Computer Engineering Commons](#)

---

Athreyas, Nihar, "Design of a Tunable Integrated Roofing Filter for Lte Bands" (2013). *Masters Theses 1911 - February 2014*. 989.  
Retrieved from <https://scholarworks.umass.edu/theses/989>

This thesis is brought to you for free and open access by ScholarWorks@UMass Amherst. It has been accepted for inclusion in Masters Theses 1911 - February 2014 by an authorized administrator of ScholarWorks@UMass Amherst. For more information, please contact [scholarworks@library.umass.edu](mailto:scholarworks@library.umass.edu).

**Design of a Tunable Integrated Roofing Filter for LTE Bands**

A Thesis Presented

by

NIHAR ATHREYAS

Submitted to the Graduate School of the  
University of Massachusetts Amherst in partial fulfillment  
of the requirements for the degree of

MASTER OF SCIENCE IN ELECTRICAL AND COMPUTER ENGINEERING

February 2013

ELECTRICAL AND COMPUTER ENGINEERING

© Copyright by Nihar Athreyas 2013

All Rights Reserved

# **Design of a Tunable Integrated Roofing Filter for LTE Bands**

A Thesis Presented

by

**NIHAR ATHREYAS**

Approved as to style and content by:

---

Dev Gupta, Chair

---

Eric Polizzi, Member

---

Hossein Pishro-Nik, Member

---

Christopher V. Hollot, Department Head  
Electrical and Computer Engineering

## **ACKNOWLEDGMENTS**

I would like to thank Prof. Dev Gupta for allowing me to work on this project and for his guidance and help. I am deeply grateful to Dr. Zhiguo Lai for his invaluable guidance and constant support throughout the course of this project. I am thankful to the University of Massachusetts, Amherst for allowing me to use the lab and other resources. I would like to express my gratitude to Prof. Eric Polizzi and Prof. Hossein Pishro-Nik for their time and for accepting to be on my thesis committee. Finally, I extend my heartfelt thanks to my parents, family and friends who have been my constant source of support throughout my time here at the University.

## ABSTRACT

### DESIGN OF A TUNABLE INTEGRATED ROOFING FILTER FOR LTE BANDS

February 2013

NIHAR ATHREYAS

B.E., M.S. RAMAIAH INSTITUTE OF TECHNOLOGY

M.S.E.C.E., UNIVERSITY OF MASSACHUSETTS AMHERST

Directed by: Professor Dev Gupta

The advent of new standards in wireless communication like the Long Term Evolution (LTE) has resulted in a need for newer and better design of receivers for wireless communication systems, the first step of which is to design a tunable integrated filter on the receiver front end.

In this work we propose a new design for a passive tunable integrated Roofing filter for LTE bands. The role of the Roofing filter is to protect the rest of the circuitry from overloading and distortions caused due to large out-of-band signals. This filter protects the rest of the circuitry and hence it gets the name *Roofing filter*.

The Roofing filter is present on the receiver front-end. The filter has a low insertion loss and a high return loss at the input. The bandwidth of the Roofing filter is around 200MHz at the highest values.

The filter uses off-chip inductors. The filter has a continuous center frequency tuning range of 2GHz from 0.7GHz to 2.7GHz, which is the allocated frequency range for LTE bands. This continuous tuning is achieved by the use of MOSFET based varactors. The filter is a narrowband filter. The design is implemented in TSMC 65nm CMOS technology.

# TABLE OF CONTENTS

	Page
ACKNOWLEDGMENTS .....	iv
ABSTRACT .....	v
LIST OF TABLES .....	ix
LIST OF FIGURES .....	x
CHAPTER	
1. INTRODUCTION .....	1
1.1 Overview.....	1
1.2 Motivation.....	2
1.2.1 Receiver Non linearity and Gain compression .....	2
1.2.2 Advantages of Roofing filter integration and Tunability.....	3
2. REVIEW OF RELATED WORK .....	5
2.1 Filter implementation.....	5
2.2 SAW filters and switched capacitor tuning .....	6
2.3 Varactor based tunable filters .....	8
2.4 Contributions of our work.....	9
3. BASIC CIRCUIT MODEL .....	11
3.1 Passive Bandpass filter design.....	11
3.2 Inductor Model.....	12
3.3 The Transfer function .....	14
4. DESIGN OF THE ROOFING FILTER USING MATLAB.....	16
4.1 Resistor Bank.....	16
4.2 Setting the Inductor value .....	16
4.3 Finding the capacitance values using MATLAB.....	18
4.4 Finding the resistance values using MATLAB.....	18
5. MATLAB EXPERIMENTAL RESULTS.....	23
5.1 Experimental Setup.....	23
5.2 Frequency Response .....	23
5.3 Comparison between the ideal and actual case.....	28



6. DESIGN OF THE ROOFING FILTER IN 65nm CMOS TECHNOLOGY .....	31
6.1 TSMC 65nm Technology .....	31
6.2 Roofing Filter Schematic .....	31
6.2.1 Inductor .....	32
6.2.2 Resistor bank and MOSFET switches .....	33
6.2.3 Use of Varactors for Tuning .....	36
6.2.1 Roofing Filter Termination, Bias Voltages and Control Voltages .....	41
7. EXPERIMENTAL RESULTS FOR THE ROOFING FILTER PRE-LAYOUT SIMULATION .....	43
7.1 Corner Simulations .....	43
7.1.1 Frequency Response .....	43
7.1.2 Insertion loss and Bandwidth .....	51
7.1.3 Parametric Analysis .....	53
7.1.4 Monte Carlo Simulations .....	58
7.1.5 Return Loss .....	60
7.1.6 Roofing Filter Linearity .....	61
8. EXPERIMENTAL RESULTS FOR THE ROOFING FILTER POST-LAYOUT SIMULATION .....	66
8.1 Parasitic Extraction and Chages to the circuit .....	67
8.2 Corner Simulations .....	71
8.2.1 Frequency Response .....	72
8.2.2 Insertion loss and Bandwidth .....	78
8.2.3 Parametric Analysis .....	81
8.2.4 Monte Carlo Simulations .....	87
8.2.5 Return Loss .....	88
8.2.6 Roofing Filter Linearity .....	89
8.2.7 Comparison of Roofing Filter Performance with existing Filters .....	92
9. CONCLUSIONS AND FUTURE WORK .....	94
BIBLIOGRAPHY .....	96

## LIST OF TABLES

Table	Page
1: 31 center frequency values and corresponding resistor values and capacitor values.....	24
2: 31 center frequency values, the corresponding actual resistor values and the switch settings to obtain these values .....	27
3: Inductor SPICE model parameters .....	33
4: Transistor sizes, Transistor on-resistance and Resistor Values .....	35
5: Transistor Sizes, Varactors, Resistor and Capacitor Values.....	40
6: Center frequencies, switch settings and Bias voltage values in TT corner.....	47
7: Center frequencies, switch settings and Bias voltage values in SS corner .....	48
8: Center frequencies, switch settings and Bias voltage values in FF corner .....	50
9: Single tone IP3 and IP5 points for the center frequencies of 1GHz and 2GHz for all three corners .....	64
10: Double tone IMD IP3 and IP5 points .....	65
11: Inductor values and SPICE parameters .....	70
12: PMOS transistors sizes, varactor sizes, resistor and capacitor values .....	71
13: Center frequencies, switch settings and Bias voltage values in TT corner.....	73
14: Center frequencies, switch settings and Bias voltage values in SS corner .....	75
15: Center frequencies, switch settings and Bias voltage values in FF corner .....	77
16: Single tone IP3 and IP5 points for the center frequencies of 1GHz and 2GHz for all three corners.....	91
17: Double tone IP3 and IP5 points for the center frequencies of 1GHz and 2GHz for all three corners.....	91
18: Comparison of the Roofing filter performance with existing filters .....	92

## LIST OF FIGURES

Figure	Page
1: RLC Bandpass Filter circuit .....	12
2: Inductor SPICE model.....	13
3: Magnitude response of the filter for ideal resistor values.....	25
4: Magnitude response of the filter for actual resistor values.....	27
5: Comparison of variation in bandwidth for ideal and actual cases .....	28
6: Comparison of variation in Insertion Loss for ideal and actual cases .....	29
7: Variation of Return loss over frequency.....	30
8: Roofing Filter Schematic.....	32
9: Variation of NMOS on-resistance with change in gate voltage .....	34
10: Variation of NMOS on-resistance with change in Transistor width .....	35
11: Equivalent circuit model of accumulation-mode MOS varactor .....	37
12: Variation of TSMC varactor capacitance with DC bias voltage .....	38
13: Simple RC network to measure the capacitance of the varactor .....	38
14: Magnitude response of the Roofing filter schematic in TT corner.....	47
15: Magnitude response of the Roofing filter schematic in SS corner .....	49
16: Magnitude response of the Roofing filter schematic in FF corner .....	50
17: Insertion loss of the roofing filter vs. Frequency.....	52
18: Bandwidth of the roofing filter vs. Center Frequency.....	53
19: Parametric Analysis: Insertion loss vs. Center Frequency in TT corner .....	55
20: Parametric Analysis: Insertion loss vs. Center Frequency in SS corner .....	55
21: Parametric Analysis: Insertion loss vs. Center Frequency in FF corner .....	56

22: Parametric Analysis: Bandwidth vs. Center Frequency in TT corner .....	57
23: Parametric Analysis: Bandwidth vs. Center Frequency in SS corner.....	57
24: Parametric Analysis: Bandwidth vs. Center Frequency in FF corner.....	58
25: Monte-Carlo Simulations for device mismatch .....	59
26: Return Loss of Roofing Filter.....	61
27: 1dB Compression point at center frequency of 1GHz.....	62
28: Roofing Filter Layout .....	67
29: Modified Roofing filter circuit .....	69
30: Magnitude Response of the Roofing Filter in TT corner.....	74
31: Magnitude Response of the Roofing Filter in SS corner .....	76
32: Magnitude Response of the Roofing Filter in FF corner .....	78
33: Variation of Insertion loss with center frequency for all 3 corners .....	79
34: Variation of Bandwidth with center frequency for all 3 corners .....	80
35: Parametric Analysis: Insertion loss vs. Center Frequency in TT corner .....	82
36: Parametric Analysis: Insertion loss vs. Center Frequency in SS corner .....	83
37: Parametric Analysis: Insertion loss vs. Center Frequency in FF corner.....	84
38: Parametric Analysis: Bandwidth vs. Center Frequency in TT corner .....	85
39: Parametric Analysis: Bandwidth vs. Center Frequency in SS corner.....	86
40: Parametric Analysis: Bandwidth vs. Center Frequency in FF corner.....	87
41: Monte-Carlo Simulations for device mismatch .....	88
42: Return Loss of Roofing Filter.....	89
43: 1dB compression point of Roofing Filter for 1GHz center frequency .....	90

# CHAPTER 1

## INTRODUCTION

### 1.1 Overview

Wireless Communication is a field that is always evolving. With the advancement in CMOS technology, wireless communication devices are becoming smaller and more powerful. There are new standards for wireless communication like 3GPP (3<sup>rd</sup> Generation Partnership Project) Long Term Evolution (LTE), LTE advanced and WiMAX.

For many years now, the goal of the telecom industry has been to achieve a new global standard for wireless communication and LTE is the closest the industry has come to achieving this standard with most of the operators supporting it. LTE will operate in various radio channel sizes ranging from 1.4MHz to 20MHz. The frequency bands allocated for LTE range from 0.7GHz to 2.7GHz [34].

The advent of these new standards in communication has resulted in a need for newer and better design of receivers for wireless communication systems. The first step of which is to design a filter on the receiver front end that can operate in all these frequency bands.

The current receivers use filter banks at the receiver front end to operate at different frequencies. These filter banks use a variety of switches to operate at different frequencies and the filters themselves are implemented in different ways. The increasing level of system integration has resulted in more functionality being built onto a single

chip. In this work we have designed and implemented a tunable, integrated filter, which can operate in the frequency range of 0.7GHz to 2.7GHz as required by the LTE bands.

## **1.2 Motivation**

### **1.2.1 Receiver nonlinearity and gain compression**

The design of a receiver in a communication system depends on a lot of factors and it essentially has to be a tradeoff between some of these factors. The smallest signals that can be processed by the receiver depends on the noise present in the system and the large signal handling of the receiver is limited by the distortions produced due to the nonlinearity of the receiver and its components [12].

The receiver process small signals that are desired and they reject very large signals that are undesired. Large signals interfere with the reception of the weak signals. One method to counter such interference is to increase the amplitude of the desired signal, which is done by increasing the transmitter output power [12]. This will result in increased power consumption and hence is not considered a practical solution.

Gain of any system can be defined as the ratio of the power available at the output to the power available at the input. Mathematically it can be defined as:

$$G = \frac{P_{OUT}}{P_{IN}}$$

$P_{out}$  is the power available to the load in watts.

$P_{in}$  is the power available from the source in watts.

Gain in decibels is given by the equation:

$$G_{db} = 10 \log \frac{P_{OUT}}{P_{IN}}$$

For an ideal system the above equation is constant for all values of input power. In an actual system the output power increases linearly with increase in the input until such a point where the distortion product energy combines with the fundamental output and this combination is observed at the output. After this point the ratio of the output power and input power ceases to be a constant. At some value of the input signal level the output signal power becomes 1dB less than the output signal power of an ideal system. This point is known as the 1-dB compression point [12].

As the input level signal increases, higher order harmonics also contribute to the output. The output power continues to deviate from the ideal behavior and eventually the input signal increases to a point where the output power of the fundamental frequency reaches a maximum value, which is called the saturation point of the system [12].

Gain compression and receiver saturation are caused due to the nonlinearity of the system. This nonlinearity can be caused by heat due to power dissipation or by overdriving the device beyond its linear region. A strong input signal, either desired or undesired, can cause receiver compression and saturation. If the compression is due to an undesired signal and if the desired signal is very small then this will lead to a decrease in Carrier-to-Noise Ratio (CNR) and which in turn will increase the bit error rate and hence the message will not be reliable [12].

The saturation and gain compression of the receivers due to strong out-of-band signals is one of the major problems in RF receivers used in wireless communication systems. In order to overcome this problem Roofing Filter is used.

### **1.2.2 Advantages of Roofing Filter integration and tunability**

Most of the receivers use Surface Acoustic Wave (SAW) filters with filter banks at the receiver front end because of their good performance. However SAW filters are not compatible with silicon integration and these filters are implemented discretely off chip. Even though these filters have good performance they occupy a lot of space and are not cost efficient. In order to reduce the space occupied and make them more cost efficient the filters have to be integrated on chip with the other blocks of the receiver. There are other advantages of integrating the filter, like reduced power consumption and increased flexibility in design [23].

The other factor that has to be taken into consideration is tuning the filter. Modern communication standards operate in multi-bands and they have flexible frequency profiles. These devices operate at multiple frequencies simultaneously and in order to operate in these multiple bands the filters should be capable of operating at different frequencies. For this reason filter banks are used in the receivers. The disadvantage of using filter banks is that for one, they do not provide continuous tuning ability and secondly they occupy a large area. The advent of LTE, a new standard of wireless communication, which has been allocated frequency bands of more than 2GHz from 0.7GHz to 2.7GHz in the form of chunks of different bandwidths, demands the need for a single filter that can be operated at all these frequencies.

This motivates us to design and implement a tunable Roofing filter at the receiver front end that has a good performance over the entire frequency range of 2GHz.



## CHAPTER 2

### REVIEW OF RELATED WORK

Filters are one of the most important components of a communication system. They are used in various stages such as baseband (BB), Intermediate Frequency (IF) and Radio Frequency (RF) in both transmitters and receivers [22]. RF band-pass filters operate on RF signals. In the receiver they are present as close to the antenna as possible and they are used to suppress out-of-band signals and hence protect the rest of the receiver circuitry from being saturated. The design of these front-end Roofing filters is complicated due to the stringent requirements of low insertion loss, narrow bandwidth and small size.

#### 2.1 Filter implementation

Various methods are used for the implementations of Band-pass filters that are used in receivers. According to Kuhn, et al. [10] they can be broadly classified based on their implementation as on-chip filters and off -chip filters. The off-chip band-pass filters can be further classified into Discrete Ceramic (DC) filters, Surface Acoustic Wave (SAW) filters, Monolithic crystal filters (MCF), and LC filters. The on-chip filters can be classified as Analog filters and Digital filters. Analog filters can be either active filters or passive filters. The passive filters use passive components like inductor (L) and capacitor (C) whereas the active filters use Transconductance-capacitors (Gm-C), Switched Capacitors and Q enhanced LC approaches.

Each of these implementations has their own advantages and disadvantages. The advantage of off chip filters is that they are very cheap and hence are used everywhere but they have the disadvantage of being large and they also consume more power. The

digital filters can be implemented on chip and they have the advantage of high precision, wide dynamic range and programmability but they are not suitable for all on-chip applications because of the need for analog anti-aliasing filters, external clocks, more chip area and need of high speed analog to digital converters [10].

The fabrication of on-chip capacitors and fabrication of on-chip inductors through planar spiral geometry [15] has led to the possibility of Passive filters being implemented on-chip. But these on chip inductors are susceptible to ohmic and eddy current losses and as a result of these losses they have a low Q-factor [16]. The other factor of concern is that they occupy a large area on chip and this is a problem especially when multiple inductors have to be used.

In [1] the authors try to overcome the disadvantages of the passive LC filters like low Q and losses due to inductor by the use of active components. These analog active filters are called Q-enhanced filters. However these filters are not suitable for handling large out-of-band signals. The on-chip inductors also suffer from series resistance losses in CMOS technology and their Q factors are very low at low frequencies [14]. The transconductance-capacitor filters are not used for RF applications in the GHz range as they have a Q dependency that is inversely proportional to the center frequency [25][6].

## **2.2 SAW filters and switched capacitor tuning**

One of the most commonly used RF Band-pass filters are based on electro acoustic devices like the Surface Acoustic Wave filters or SAW filters. These filters are electromechanical devices in which a piezoelectric crystal converts an electrical signal to a mechanical wave. This mechanical wave is delayed as it propagates and it is converted back to an electrical signal with the help of interdigital electrodes [24]. The major

disadvantage of SAW band-pass filters is that they have high insertion losses, complex design, fixed frequency of operation and they are not easily integrated on chip.

Some of these problems have been addressed in the recent past. In [17] Novgorodov et al. have designed and implemented a ladder-type SAW Band-pass filter based on low temperature co-fired ceramic (LTCC) substrate. It is designed for a center frequency of 2.4-2.5GHz. The design used two input/output inductors and three additional inductors that are integrated with the ceramic. A maximum insertion loss of -1.5dB at a frequency range of 2.4-2.5 GHz was obtained. Return losses of around 17dB were achieved in the pass-band. Fixed frequency of operation is a major disadvantage of the SAW band-pass filters. In [5] in order to achieve tunability of center frequency the author proposes a low-loss SAW band-pass filter with MEMS switches. The MEMS switches have a high linearity and low power consumption. In this design, to achieve tunability from 400-478 MHz, SAW filters banks with 8 channels are used. The insertion losses obtained are in the range of 3.2dB with pass-band ripple of 1dB. The tuning range of each MEMS switch is around 27.4 MHz. The control voltages are around 5V and power consumption is around 6mW. The design also occupies a large area. These factors make the integration of the chip difficult and incompatible with CMOS design. Again the major problem associated with the SAW filters is the difficulty in achieving wide tunability of center frequency.

In [18] Oualkadi et al. have proposed a new high-Q pseudo switched-capacitor CMOS LC band-pass filter. The tunability is achieved using switched capacitance circuit. According to the authors this circuit was designed to replace SAW filters in wireless broadband applications. In this design 8 branches of the switched capacitors are used

which are turned on and off by the N-channel MOSFET. A command circuit consisting of a voltage controlled oscillator implemented using XOR gates are used to control these switches. The circuit was fabricated in 0.35 $\mu$ m CMOS technology. A tuning range of 240MHz to 525 MHz was obtained. Insertion loss of 2dB was observed. From this we realize that tunable band-pass filters with good performance can be integrated on chip. The disadvantage of using the switched capacitance filter is that the filter has more noise at the output i.e. random noise and clock feed-through, than normal active filters. The tuning range that can be achieved with the use of switched capacitance circuits is generally of the order of a few decades. In order to obtain a continuous tunability of the center frequency over a wide range, varactors or variable capacitors have to be used. There has been some work done in the design of tunable band-pass filters based on varactors.

### **2.3 Varactor based tunable filters**

Varactors are the devices of choice for the purpose of tuning a band-pass filter continuously. Varactors or variable capacitors are voltage-controlled capacitors. CMOS processes generally use either p-n junction diode varactors or MOSFET based varactors.

In [7] the authors propose an electronically tunable microwave band-pass filter. Varactor diodes are used for the purpose of tuning. These varactor diodes use the change in the depletion layer capacitance as a function of the applied bias voltage. The filter itself was a comb line filter. The proposed design was able to achieve a tuning range of 1700MHz from 3.2 to 4.9 GHz with a maximum pass-band insertion loss of 6dB and minimum pass-band return loss of 8dB. The bandwidth variation across the entire tuning range was found to be around 12.3 percent. With this novel design the authors gave way

to the development of electronically tunable band-pass filters. In [2] a similar tunable band-pass filter is implemented. The tuning element used is commercially available reverse biased varactor diodes. The filter was fabricated on RT/Duriod with a dielectric constant of 2.2. A tuning range of 700MHz to 1.33 GHz was obtained. A return loss of -10dB was observed over the entire tuning range of 1.3 GHz. The insertion losses obtained were around 3dB for center frequencies of more than 1GHz. At center frequencies below 1GHz low bandwidth and higher insertion losses were observed. The limiting factor for insertion loss in both the cases was the series resistance of the varactor diodes.

## **2.4 Contributions of our work**

With the growing demand for faster and better forms of communication systems and the wireless communication standards heading towards 4G, there is a demand for better design of communication systems. In this work we have designed and implemented a passive tunable *Roofing filter* with a low insertion loss that can be integrated on a chip. The filter has a high return loss and a narrow bandwidth. The term ‘narrow’ is relative. Since the center frequency will be in the GHz range, the bandwidth of the filter is of the order of a few hundred MHz’s. Passive filter design is chosen because the filter will be used to reject large out-of-band signals and because of the high frequency of operation. The filter uses off chip inductors as opposed to on chip inductors as the on chip inductors occupy a large area, have a low Q-factor and they are also subject to losses. The filter is continuously tunable in the frequency range of 0.7GHz to 2.7GHz in correspondence with the allocated frequency bands for LTE. The tunability is achieved with the help of MOSFET based variable capacitors or varactors.

The goal of the *roofing filters* is to reduce the pass band so that the overloading and distortions of the following amplifiers and mixers of the receiver are reduced. This filter protects the rest of the circuitry from the strong out-of-band signal or *it acts as a roof*. Hence it gets the name *Roofing filter*.

## CHAPTER 3

### BASIC CIRCUIT MODEL

#### 3.1 Passive Band-pass filter design

Receiver Front-end is a term that is used for all the circuitry that is present between the antenna and the first IF filter. The receiver front-end generally consists of the following blocks:

- 1) Impedance matching circuits to transfer maximum power from the antenna.
- 2) A Bandpass filter to reject the noise and large out-of-band signals.
- 3) An RF amplifier called Low Noise Amplifier (LNA).
- 4) Mixer to mix the incoming RF signal with the local oscillator signal to convert it into IF signal.

The Roofing filters are generally the first filters on the receiver front end and they are placed as close to the antenna as possible. They are band-pass filters, which are used to eliminate or suppress large out-of-band signals. Since the requirement is to handle large signals, a passive filter design is chosen for our work. Passive filters can either be electro acoustic filters or LC filters [10]. Electro acoustic filters are not compatible with silicon integration, they have a fixed frequency of operation and require external matching elements [15]. Hence a passive LCR filter is the apt choice for our design.

There are two categories of band-pass filters: wideband and narrowband filters. A filter is called a wideband filter if the upper and lower cutoff frequencies are more than an octave apart i.e. if the upper cutoff frequency is more than twice the lower cutoff frequency. If the upper and lower cutoff frequencies are less than an octave apart, then

they are called narrowband band-pass filters. The filter we are proposing here is a narrowband band-pass filter.

Figure 1 below shows the basic circuit model of the proposed Roofing filter. It is a passive RLC band-pass filter in which the inductor and the capacitor are in parallel with the resistor in series. The output is taken across the parallel LC combination. This circuit forms the basis for the design of the roofing filter.

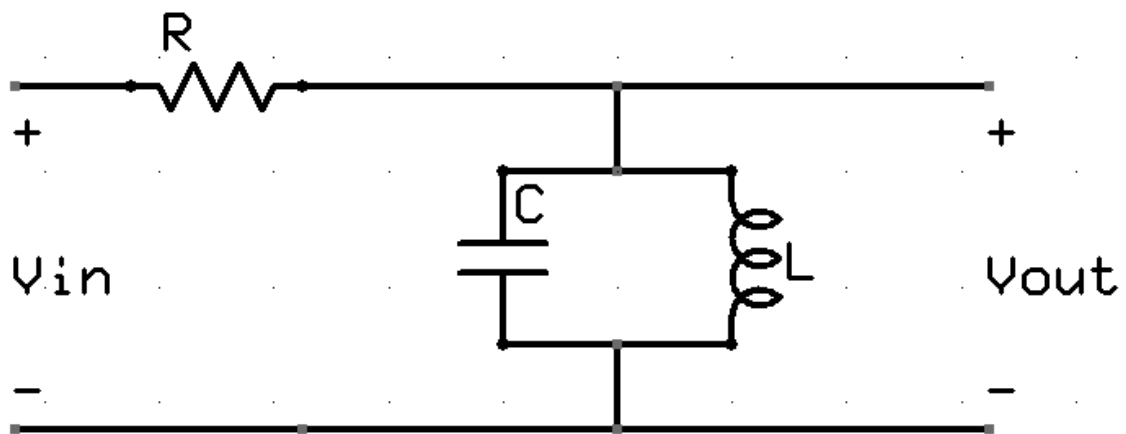


**Figure 1: RLC Band-pass filter circuit**

### 3.2 Inductor Model

Most of the passive on-chip LC band-pass filters use on chip inductors and as a result suffers from low Q-factor and eddy current losses [16]. On chip inductors also occupy a large area. In order to overcome these disadvantages we will be using off-chip inductors in our proposed roofing filter design. The advantages of using an off chip inductors is that we can get high Q-factors at all frequencies of operation. The losses of the inductor will be minimal.



In order to make the circuit as realistic as possible and in order to take into account the parasitic resistance and capacitance of the inductors we use the SPICE model [28] of the inductor while doing the calculations and in our simulations.

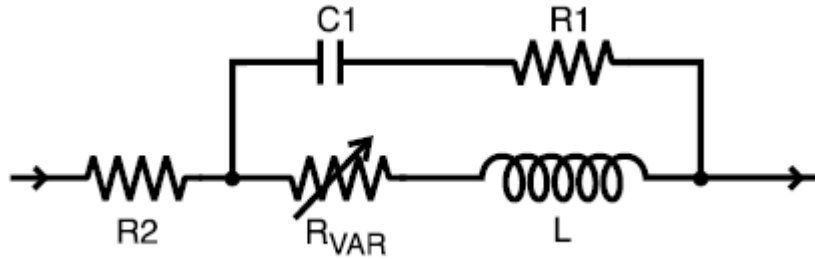


**Figure 2: Inductor SPICE model [28]**

The resistor  $R_{VAR}$  shown in the above spice model is a variable frequency dependent resistor. The dependence of the resistor on frequency is given by:

$$R_{VAR} = k \cdot \sqrt{f}$$

Where,  $k$  is a constant and it depends on the inductor being used and  $f$  is the frequency in Hz [28]. This frequency dependent resistor relates to the skin effect experienced by the inductors [28]. In an ideal case an inductor is a purely reactive device but in reality they have some resistance as well. Hence the impedance of any real inductor will be a complex combination of resistance and inductive reactance. This is further complicated by skin effect, which is the tendency of the AC current to flow on the surface of the conductor rather than flow in the middle. In order to account for the losses due to skin effect the variable resistor is used.

The impedance of the inductor can be calculated from the spice model as:

$$Z = (R_1 + X_{C1} \parallel R_{VAR} + X_L) + R_2$$

Where,  $X_L = j2\pi fL$      $X_{C1} = 1/j2\pi fC1$      $f = 1/2\pi\sqrt{LC}$

This gives us the impedance of the inductor, which will have a real part  $R_L$  and an imaginary part  $X_L$ .

### 3.3 The Transfer function

A transfer function is a mathematical representation of the relationship between the input and output of a system. Transfer functions are generally used in the analysis of single input single output systems. In its simplest form for continuous time input signal  $x(t)$  and output signal  $y(t)$ , the transfer function is a linear mapping of the Laplace transform of the output  $Y(s)$  to that of the input  $X(s)$ :

$$Y(s) = H(s)X(s)$$

$$H(s) = \frac{Y(s)}{X(s)}$$

$H(s)$  is the transfer function of the system.

The transfer function of the band-pass filter can be calculated in the Laplace domain.

The impedance of a capacitor is given by  $Z_C = 1/j2\pi fC$  and the impedance of an inductor is given by  $Z_L = j2\pi fL$ .

$$Z_C = 1/j2\pi fC \text{ and } Z_L = j2\pi fL$$

Substituting  $\omega = 2\pi f$  in  $Z_L$  and  $Z_C$  we get

$$Z_C = 1/j\omega C \text{ and } Z_L = j\omega L$$

Taking the Laplace transform of the impedance of the inductor and the capacitor we get

$$Z_C = 1/sC \text{ and } Z_L = sL$$

$$V_{OUT}(s) = \frac{Ls}{RLCs^2 + Ls + R} V_{IN}(s)$$

$$\frac{V_{\text{OUT}}(s)}{V_{\text{IN}}(s)} = \frac{\frac{s}{RC}}{s^2 + \frac{s}{RC} + \frac{1}{LC}}$$

The above equation gives the transfer function the LCR band-pass filter.

## CHAPTER 4

### DESIGN OF THE ROOFING FILTER USING MATLAB

We begin the design process by choosing an inductor with a particular inductance value. Since the inductor we are using in our design is off-chip, it will have a fixed value. Once the inductor is chosen and its value is fixed, all the other device parameters are calculated around this value. The next step in the design process is to calculate the capacitance values. Since we know the center frequencies at which the filter is going to operate and we also know the inductance value, the capacitance values can be calculated. The next step would be to calculate the resistance values. The most important point to be considered at this stage is that the proposed filter is a continuously tunable filter from 0.7GHz to 2.7GHz i.e. the filter should be able to operate at any frequency between these two frequencies.

#### **4.1 Resistor Bank**

The continuous tunability of the proposed filter can be achieved by the use of a varactor, but for each of the capacitance value calculated there will be a resistance value that can be calculated. Since we cannot have these many resistors, the proposed idea is to have a resistor bank with 5 resistor switches. By using different combinations of these 5 resistors in parallel we can get 31 different resistance values. These 31 different values are used to cover the entire frequency range of 2GHz. We have chosen the number of resistor switches to be 5 because it sets the bandwidth of the filter. The calculation of the resistance and capacitance values is done using MATLAB.

#### **4.2 Setting the inductor value**

Since we need a starting point, we first choose the number of resistor switches to be 5. This gives us  $2^5$  i.e. 32 different combinations of resistor values, of which the 'all zero' combination is ignored as it gives an infinite resistance. So effectively we have 31 different resistance values. The entire frequency range of interest i.e. 0.7GHz to 2.7GHz is divided into 31 equal divisions. These frequencies will act as the center frequencies for our calculations. The 31 center frequencies in GHz are: 0.7000, 0.7667, 0.8333, 0.9000, 0.9667, 1.0333, 1.1000, 1.1667, 1.2333, 1.3000, 1.3667, 1.4333, 1.5000, 1.5667, 1.6333, 1.7000, 1.7667, 1.8333, 1.9000, 1.9667, 2.0333, 2.1000, 2.1667, 2.2333, 2.3000, 2.3667, 2.4333, 2.5000, 2.5667, 2.6333, 2.7000.

The number of switches being used also sets the bandwidth of the filter. Since we have 31 center frequencies, at each of these frequencies the Roofing filter should have a minimum bandwidth of  $2\text{GHz}/31$  i.e. 64.5MHz in order to cover the entire frequency range of 2GHz. Hence the bandwidth of this ideal Roofing filter will be 64.5MHz.

In order to choose an inductor value, we take the geometric mean of all the 31 center frequencies calculated. The geometric mean was found 1.603GHz. We next fix the capacitance value to an arbitrary value of 1pF. Since we know the center frequency and the capacitance value we can calculate the inductance value using  $L=1/4\pi^2f^2C$ . The inductance value we obtained was 9.89nH. Hence we choose to use a 10nH inductor. The off chip inductor we are using is from Coilcraft Inc. From the data sheets we obtain the values of the resistor and capacitor present in the spice model of the inductor. From these values the impedance of the inductor is calculated for the frequencies ranging from 0 Hz to 10 GHz in steps of 100 KHz. The impedance of the inductor will have a real part  $R_L$  and an imaginary part  $X_L$ .

In order to calculate the inductance values at frequencies ranging from 0GHz to 10GHz we only need the reactance part of the impedance of the inductor. Hence from the reactance component obtained we recalculate the inductance values at the corresponding frequencies, which gives us 10000 new inductor values.

#### **4.3 Finding the capacitance values using MATLAB**

The 31 center frequencies obtained earlier are the frequencies of interest for our design. The capacitance values have to be calculated for these values of the center frequency. For that we need the inductance values at these center frequencies. While the ideal inductance values were calculated, they were done so for frequencies in steps of 100 KHz starting from 0 till 10GHz. However the inductance values needed are different from what we have calculated as the frequencies of interest are not exact multiples of 100 KHz. In order to find the inductance values at these frequencies we use a cubic spline interpolation in MATLAB. Using this process unique cubic polynomial is fitted between data points such that the entire curve appears to be smooth and continuous [13]. This interpolation gives us the inductance values at the desired frequencies. Knowing the inductance value and the center frequencies the corresponding capacitance values are calculated as  $C=1/4\pi^2f^2L$ .

#### **4.4 Finding the resistance values using MATLAB**

The inductor value is known and the capacitance values have been calculated and with these the center frequency of the Roofing filter can be fixed at any one of the 31 values that have been calculated. The only unknown in the circuit is the resistance values. The resistance values determine the bandwidth and the magnitude of the frequency response of the circuit.

In order to calculate the resistance values we first start by calculating the output impedance and the input impedance of the Roofing filter. The output impedance is

$$Z_{OUT} = \frac{(X_L - jR_L)X_C}{R_L + j(X_L - X_C)}$$

$$Z_{IN} = \frac{RR_L + X_LX_C + j(R(X_L - X_C) - R_LX_C)}{R_L + j(X_L - X_C)}$$

From the equations for  $Z_{OUT}$  and  $Z_{IN}$  we find the value of  $R$ , which is the unknown. Here  $X_L$  is the reactance of the inductor,  $X_C$  is the reactance of the capacitor and  $R_L$  is the resistance of the inductor.

The ratio of  $Z_{OUT}$  and  $Z_{IN}$  gives the insertion loss of the filter. The insertion loss of a filter is defined as the loss of signal power resulting from the insertion of a device and it is usually expressed in dB [20]. It is slightly different from signal attenuation because it does not take into consideration the effects of the devices that were already present like signal attenuation due to impedance mismatch.

$$IL = 20 \log \frac{|Z_{IN}|}{|Z_{OUT}|}$$

$$\frac{|Z_{OUT}|}{|Z_{IN}|} = \frac{\sqrt{(X_L^2 X_C^2 + R_L^2 X_C^2)}}{\sqrt{((RR_L + X_L X_C)^2 + (R(X_L - X_C) - R_L X_C)^2)}}$$

$$10^{(-\frac{IL}{20})} = \frac{\sqrt{(X_L^2 X_C^2 + R_L^2 X_C^2)}}{\sqrt{((RR_L + X_L X_C)^2 + (R(X_L - X_C) - R_L X_C)^2)}}$$

$$\text{Let } 10^{-\frac{IL}{20}} = b$$

Solving the above equation we get a 2<sup>nd</sup> order polynomial in R with the following coefficients

$$a_2 = R_L^2 + (X_L - X_C)^2$$

$$a_1 = 2R_L X_C^2$$

$$a_0 = (b^2 - 1)(X_L^2 X_C^2 + R_L^2 X_C^2)$$

These 3 coefficients form the basis for solving the polynomial in R. Solving this polynomial gives us 31 different resistance values at the corresponding center frequencies. Since we have fixed the number of resistor switches to be 5, we have to now select the 5 resistor switches such that different combinations of the 5 switches give us the resistance values that are as close as possible to the ideal resistance values.

In order to design the resistor bank we use an optimization algorithm, which will give us an optimum value of resistor R and an optimum value of a multiplier  $\alpha$ . The 5 resistance values of the resistor bank will be R,  $\alpha R$ ,  $\alpha^2 R$ ,  $\alpha^3 R$ ,  $\alpha^4 R$ .

**The pseudo code of the algorithm is presented below.**

*Pseudo Code:*

```

R_N=Min(R31)_Max(R31)_Interval()
 $\alpha$ _N = Value_interval()
{
  A = Binary_value
}
{
  {
    R_N1=R_N* ( $\alpha$ _N[0 1 2 3 4])
    R_av = A*R_N1_parallel
    {
      Error() = min(abs(R31-R_av)/max(R31))
    }
  }
}
[Error1,Index1] = min(Error)
[Error2,Index2] = min(Error1)
R_optimum = R_N(Index1(Index2))

```



$$\begin{aligned}
&\alpha_{\text{optimum}} = \alpha_{\text{N}}(\text{Index}_2) \\
&R_{\text{final}} = R_{\text{optimum}} * (\alpha_{\text{optimum}}^{[0\ 1\ 2\ 3\ 4]}) \\
&\{ \\
&\quad [\text{Error}_{\text{K}}, \text{Index}_{\text{K}}] = \min(\text{abs}(R_{31} - R_{\text{final}}) / \max(R_{31})) \\
&\quad R_{31\_NEW} = R_{\text{final}}(\text{Index}_{\text{K}}) \\
&\}
\end{aligned}$$

From the 31 resistance values that have been calculated the minimum resistance value and the maximum resistance value is picked. This minimum value and the maximum value form an interval, which is divided into 100 equal divisions. The value of the multiplier  $\alpha$  is fixed to be any arbitrary value. Here we fix it between 1 and 3. The interval between 1 and 3 is also divided into 100 equal divisions. Since there are 5 resistor switches in parallel, the resistors can be combined in 31 different ways which are given by the binary values from 00001 to 11111, where a 0 represents a switch being OFF and a 1 represents a switch being ON. These binary values are stored in a matrix. There are 2 loops running one inside the other. The outer loop first selects a value of the resistor. The second loop runs through all the values of  $\alpha$  in the interval. The resistor is multiplied by different powers of  $\alpha$  and then added according to the 31 different combinations and these values are stored. Then these values are compared with the original resistor values and the minimum of the magnitude of their difference divided by the maximum value (relative error) and their corresponding indices are stored as error function and index respectively. This process is repeated for all the 101 resistance values. Now we have a 101 x 101 matrix of error function and indices. The minimum value of each column and its corresponding row number is taken. This will give the resistance values with the least errors. The minimum value of these 101 error functions will give the

value of the optimum value of  $R$  and from the corresponding index we obtain the value of the multiplier  $\alpha$ .

The next step is to use these 5 resistors to obtain the 31 resistance values, which are as close as possible to the ideal resistance values. The same procedure is followed. The 5 resistor values are combined in 31 different ways and they are compared with the original 31 resistance values. The magnitude of the difference divided by the maximum value gives us error values. The minimum of this function will give us the required combinations to obtain the 31 resistance values from the 5 resistors.

## CHAPTER 5

### MATLAB EXPERIMENTAL RESULTS

#### 5.1 Experimental Setup

We have used the MATLAB tool to simulate the design of our Roofing filter and evaluate the performance of the filter. As mentioned in the previous section we have also used it to calculate the optimal parameters for our design. Even though MATLAB simulations can be considered fairly ideal, we have tried to make the simulations as close to the real world as possible by taking into account the different losses that might be experienced by the filter like the losses due to insertion of the filter into the system, which is called the insertion loss.

#### 5.2 Frequency Response

Frequency response is the quantitative measure of the output of a system in response to an input or a stimulus. The frequency response has two parts, the magnitude response and the phase response, both of which are measured as a function of frequency. Here we are interested in the magnitude response of the filter.

In any system, impedance mismatch leads to reflections, which results in a loss of signal power. In order to avoid this, impedance matching is done. Reflections are least when the load impedance is equal to the source impedance. We have taken this into consideration while performing our simulations. We have considered  $50\Omega$  source impedance while performing our simulations.

The table below shows the 31 center frequencies and their corresponding resistor values and capacitance values for an inductance value of  $10\text{nH}$ , obtained from MATLAB.

<b>Center Freq(GHz)</b>	<b>Resistor Value (K<math>\Omega</math>)</b>	<b>Capacitor Value(pF)</b>	<b>Center Freq(GHz)</b>	<b>Resistor Value (K<math>\Omega</math>)</b>	<b>Capacitor Value (pF)</b>
0.7000	0.1385	5.123	1.7667	0.7824	0.766
0.7667	0.1643	4.264	1.8333	0.8373	0.708
0.8333	0.1922	3.602	1.9000	0.8935	0.656
0.9000	0.2221	3.081	1.9667	0.9511	0.609
0.9667	0.2540	2.665	2.0333	1.0100	0.567
1.0333	0.2879	2.326	2.1000	1.0699	0.528
1.1000	0.3238	2.047	2.1667	1.1309	0.494
1.1667	0.3615	1.815	2.2333	1.1928	0.462
1.2333	0.4012	1.619	2.3000	1.2555	0.433
1.3000	0.4427	1.453	2.3667	1.3188	0.406
1.3667	0.4861	1.310	2.4333	1.3827	0.382
1.4333	0.5313	1.187	2.5000	1.4470	0.359
1.5000	0.5782	1.080	2.5667	1.5115	0.339
1.5667	0.6268	0.986	2.6333	1.5761	0.319
1.6333	0.6771	0.903	2.7000	1.6407	0.301
1.7000	0.7290	0.830			

**TABLE 1: 31 Center frequency values and corresponding Resistor and Capacitor values**

From the transfer function of the Roofing filter obtained by taking the ratio of  $Z_{OUT}$  to  $Z_{IN}$ , magnitude response of the roofing filter is calculated. The magnitude response in dB is obtained as  $20\log_{10}|H(f)|$ . Since the ratio of  $Z_{OUT}$  to  $Z_{IN}$  gives the insertion loss, the magnitude response represents the insertion loss of the roofing filter in dB.

Figure 3 shows the magnitude response of the filter for an inductance value of 10nH and the IL set at 1dB. The resistor values used are ideal i.e. 31 different resistor values are used. From the figure it can be seen that there are 31 curves, at the center frequencies ranging from 0.7GHz to 2.7GHz. The insertion loss is found to be fairly constant throughout the entire frequency range. There is an increase in bandwidth as the frequency increases.

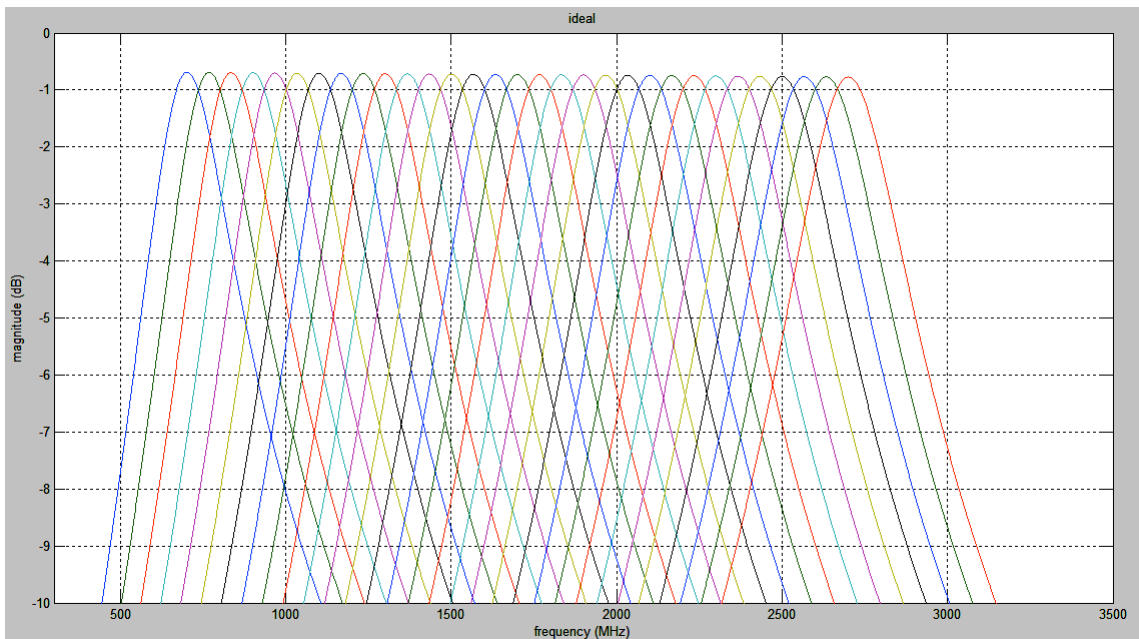


**Figure 3: Magnitude response of the filter for ideal resistor values**

The actual resistance values are calculated from the optimization algorithm in MATLAB. Since we have used 5 resistor switches, we obtain the 5 resistance values and these 5 resistance values are used in different combinations to obtain 31 resistance values. The 5 resistance values for an inductance of 10nH are: 0.3037K $\Omega$ , 0.6013K $\Omega$ , 1.1907K $\Omega$ , 2.3575 K $\Omega$ , 4.6679 K $\Omega$ .

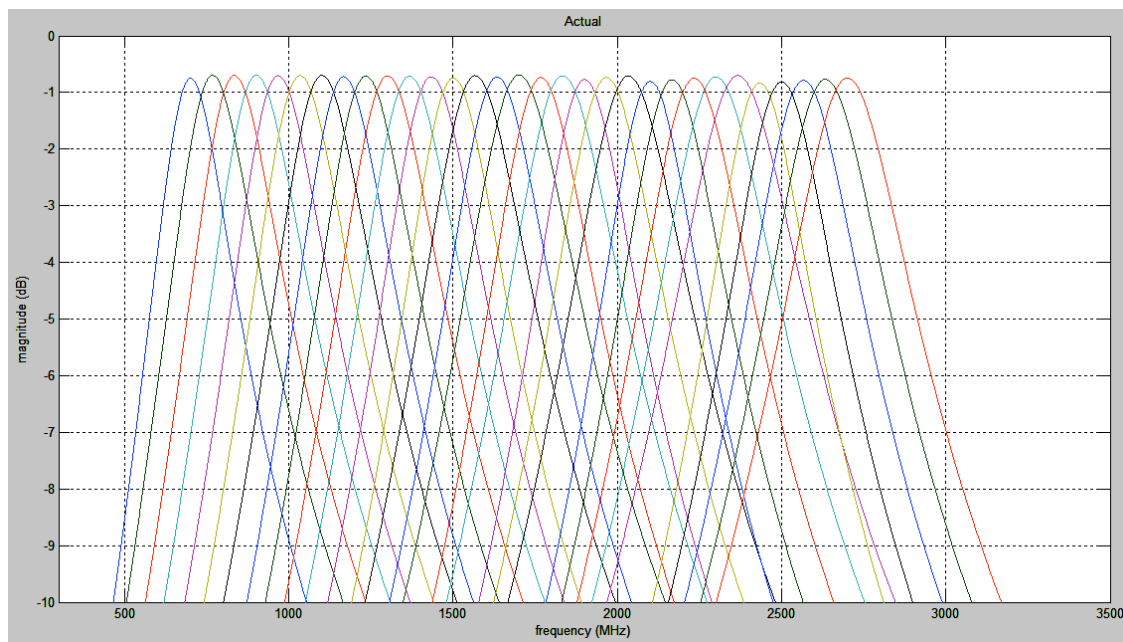
The table below gives the 31 actual resistance values and the corresponding switch settings needed to produce these 31 values by combining the 5 resistance switches in parallel. In the switch settings a ‘0’ represents a switch being off and a ‘1’ represents a switch being on, with the most significant bit (MSB) being assigned to the resistor with least value and the least significant bit (LSB) being assigned to the resistor with the maximum value.

<b>Center Freq(GHz)</b>	<b>Switch Setting</b>	<b>Resistance Value(KΩ)</b>	<b>Center Freq(GHz)</b>	<b>Switch Setting</b>	<b>Resistance Value(KΩ)</b>
0.7000	11111	0.1554	1.5667	01000	0.6013
0.7667	11101	0.1664	1.6333	00111	0.6765
0.8333	11001	0.1934	1.7000	00111	0.6765
0.9000	10110	0.2195	1.7667	00110	0.7911
0.9667	10011	0.2544	1.8333	00110	0.7911
1.0333	10001	0.2852	1.9000	00101	0.9487
1.1000	01111	0.3183	1.9667	00101	0.9487
1.1667	01101	0.368	2.0333	00101	0.9487
1.2333	01100	0.3996	2.1000	00100	1.1907
1.3000	01011	0.4345	2.1667	00100	1.1907
1.3667	01010	0.4791	2.2333	00100	1.1907
1.4333	01001	0.5327	2.3000	00100	1.1907
1.5000	01000	0.6013	2.3667	00100	1.1907

Center Freq(GHz)	Switch Setting	Resistance Value(K $\Omega$ )	Center Freq(GHz)	Switch Setting	Resistance Value(K $\Omega$ )
2.4333	00011	1.5664	2.6333	00011	1.5664
2.5000	00011	1.5664	2.7000	00011	1.5664
2.5667	00011	1.5664			

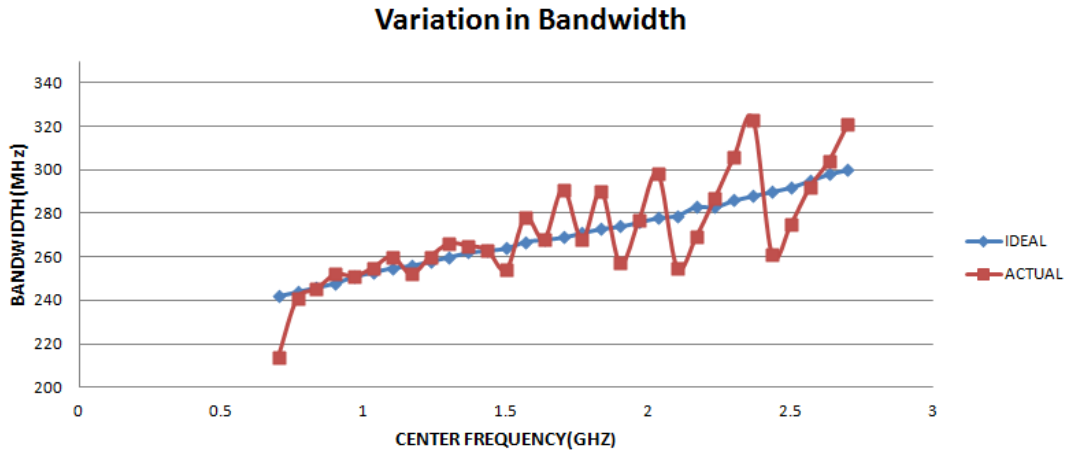
**TABLE 2: 31 Center frequency values, the corresponding actual resistor values and the switch settings to obtain these values**

Figure 4 shows the magnitude response of the filter for the same inductance and IL value but instead of using the 31 different resistor values, the 5 resistance switches are used in combinations to get the 31 resistance values. These plots are called the actual plots. In these plots also the insertion loss is observed to be almost constant throughout the entire frequency range. However there are slight variations in bandwidth as compared to the ideal case.



**Figure 4: Magnitude response of the filter for actual resistor values**

### 5.3 Comparison between the ideal and actual case



**Figure 5: Comparison of variation in bandwidth for ideal and actual cases**

Figure 5 shows the variation in bandwidth for ideal case where 31 different values of resistances are used and the actual case where the 5 resistors are used to obtain the 31 resistance combinations. In the ideal case we can see that the increase in bandwidth is almost linear whereas in the actual case there are fluctuations in bandwidth. This can be attributed to the fact that since only 5 resistors are being used to obtain the 31 different values, exact resistance values to match the ideal case cannot be obtained and hence the nearest value of the resistance available is used. The actual roofing filter will have stringent constraints about the bandwidth requirements. In order to reduce the bandwidth we can increase the inductance value. Increasing the number of resistor switches can also help in bandwidth reduction as more accurate values of resistances can be obtained. Figure 6 shows the variation of insertion loss of the filter with respect to change in center frequency. It can be seen from the figure that in the ideal case there is a monotonous decrease in the insertion loss whereas in the actual case with the use of 5 switches for resistors, there are fluctuations. The total variation in insertion loss



throughout the entire frequency range is 0.082dB in the ideal case and it is 0.144dB in the actual case.

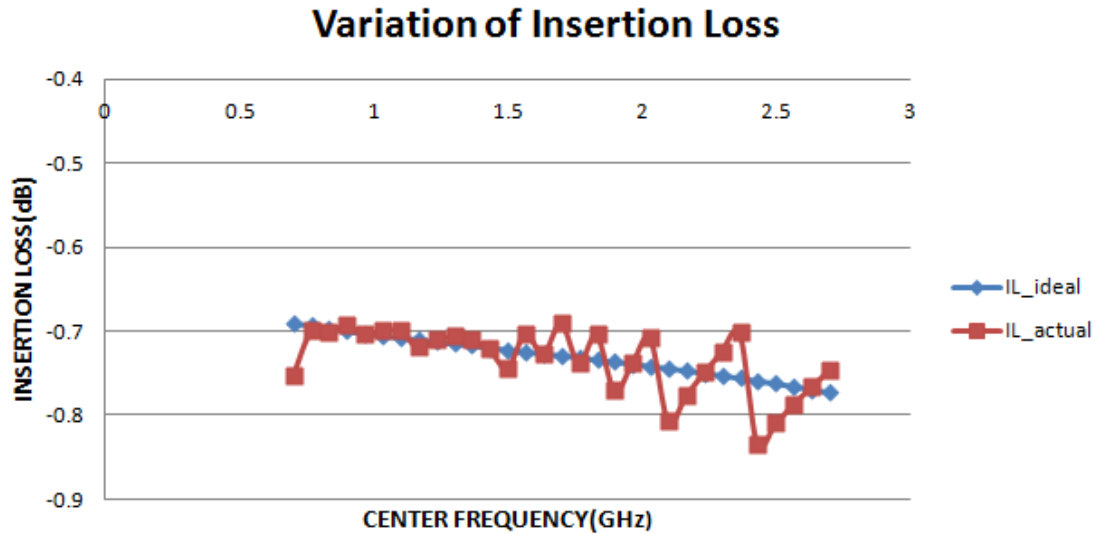


**Figure 6: Comparison of variation in Insertion Loss for ideal and actual cases**

Another parameter used to measure the performance of a filter is the return loss. It is defined as the loss of signal power resulting from reflections caused due to impedance mismatch. It is generally expressed in dB. The ratio of the reflected wave  $V_r$  to the incident wave  $V_i$  is called reflection coefficient  $\Gamma$ . If  $Z_L$  is the load impedance and  $Z_S$  is the source impedance then the reflection coefficient is given by

$$\Gamma = \frac{Z_L - Z_S}{Z_L + Z_S}$$

$$RL = -20 \log |\Gamma|$$

Here we have considered a source impedance of 50 ohm that has to be matched with the load impedance. The plots is for the inductance value set at 10nH and the IL value set at 1dB. Thus a large positive return loss indicates that the reflected power is very small compared to incident power. Figure 7 shows the Return loss at the input over

the entire range of frequencies. From Figure 7 it can be observed that the lowest return loss is at 0.7GHz and it is around 36.48dB.

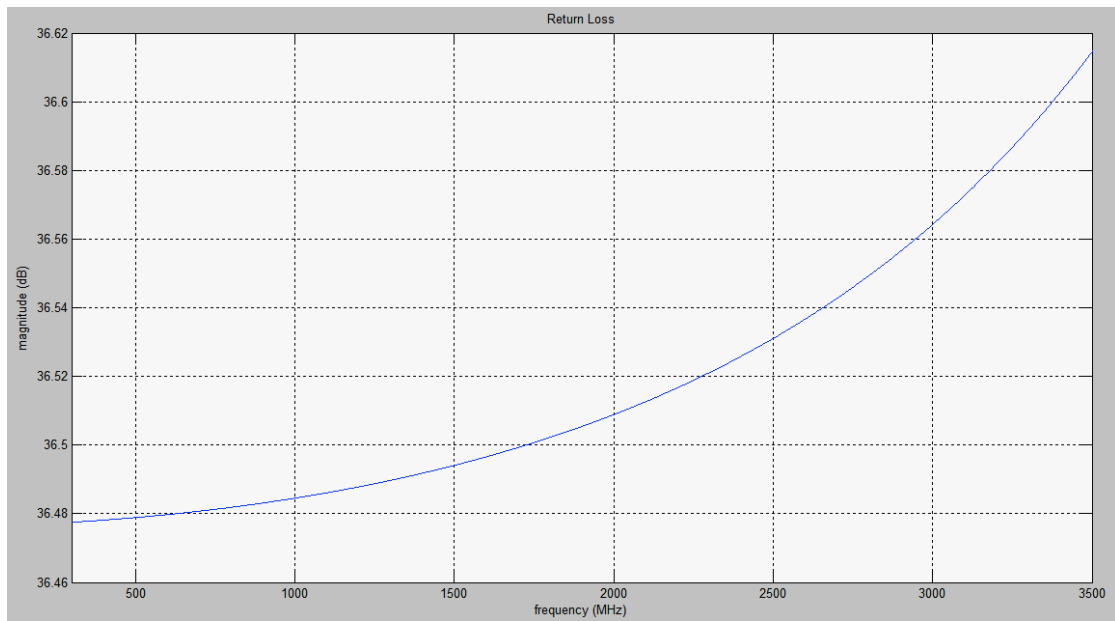


**Figure 7: Variation of Return loss over frequency**

## CHAPTER 6

### DESIGN OF THE ROOFING FILTER IN 65nm CMOS TECHNOLOGY

The proposed design shows promising results and since we are interested in building an on-chip filter the next logical step would be to implement it in a standard CMOS technology. We have implemented our design in TSMC 65nm CMOS technology. The tool used for the design is Cadence®.

#### 6.1 TSMC 65nm Technology

TSMC's 65nm CMOS technology is best suited for our design purposes. It has 30% to 50% speed improvement over the 90nm technology. It provides multiple threshold voltage architectures and also a wide operating voltage range from 0.9V to 1.26V [33]. The TSMC 65nm library has a wide variety of MOSFETs that can be used. It also provides the options of RF transistors for high frequency operation.

TSMC 65nm library also provides different types of MOSFET based varactors, which are very critical for our design.

#### 6.2 Roofing Filter Schematic

The Roofing filter design was tested using MATLAB. The resistance and capacitance values obtained from MATLAB are used to implement the design in CMOS technology. Figure 8 shows the schematic of the Roofing filter. The filter is a passive LCR filter. The main components of the circuit are the inductor (L1), varactors (C7 to C11) and resistors of the resistor bank (R1 to R5). By varying the capacitance value the center frequency of the filter can be tuned anywhere between 0.7GHz and 2.7GHz. This is accomplished with the help of varactors. For an inductance value of 10nH the capacitance values vary from 5.123pF for 0.7GHz center frequency to 0.301pF for

2.7GHz center frequency. In order to obtain any of the capacitance values in between these points the varactors are tuned to that particular value. A single varactor will not be able to achieve such a wide tuning range. Hence we will be using multiple varactors which can be turned on and off with the help of switches.

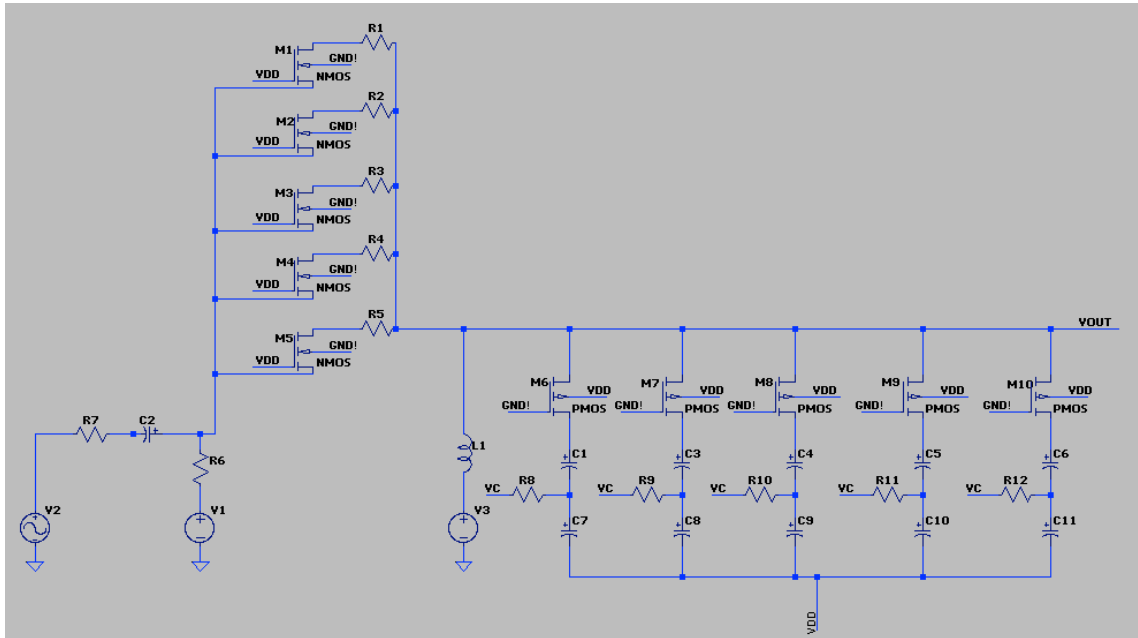


**Figure 8: Roofing filter Schematic**

### 6.2.1 Inductor

The first step in the design of the Roofing filter is choosing the inductor value. Here again we use the spice model of the inductor in order to incorporate various effects experienced by the inductor. The inductor value is a tradeoff between the bandwidth requirements and the total frequency range that has to be achieved i.e. higher the inductor value lower is the bandwidth but the frequency at which the circuit can operate is limited. In the design of the roofing filter, the frequency range of the circuit is fixed to be between 0.7GHz to 2.7GHz. We design the filter to have a bandwidth of around 200MHz but it

has to be noted that the roofing filter is used to eliminate large out of band signals. This implies lesser the bandwidth of the filter, better is its performance. Once the inductor value is fixed the other device parameters are obtained from the datasheets.

Table 3 gives the parameters of the inductor we have used for our simulation. The inductor value was fixed at 19nH and the corresponding resistance and capacitance values of the spice model were obtained from the datasheets. This particular inductor value was chosen because it gave us the best bandwidths while allowing us to attain the frequency of operation.

Inductor Model	Coilcraft 0302CS
Inductance Value	19nH
R1 Value	18.86 $\Omega$
R2 Value	1.698 $\Omega$
C Value	0.040pF
k	1.18E-5
Rvar Value	0.373 $\Omega$

**TABLE 3: Inductor SPICE model parameters**

### 6.2.2 Resistor Bank and MOSFET switches

In the design of the Roofing filter we are using a resistor bank consisting of 5 resistors, which can be combined, in parallel to obtain 31 different resistance values. In order to get 31 different combinations we should be able to connect and disconnect these resistors. This is achieved with the help of NMOS transistor switches connected to the resistors. The 65nm TSMC library provides us with a wide selection of MOSFETs with

different operating voltages and different threshold voltages. While designing the Roofing filter circuit and using the MOSFET switches the important things to be considered are the resistance and the capacitance of the MOSFET itself. While using the MOSFET to control the resistors, the resistor values can be decreased by the amount that will be compensated by the MOSFET switches. This is done because the MOSFETs have an internal resistance of their own when they are turned on.

Figure 9 shows the variation of the NMOS transistor on-resistance with respect to change in the gate voltage for a fixed transistor width of  $10\mu\text{m}$  and gate length of  $60\text{nm}$ . When the gate voltage is  $0\text{V}$  the transistor is off and the transistor presents a very high resistance. As we increase the gate voltage transistor begins to turn on and after it crosses the threshold voltage the resistance begins to drop and reaches saturation at around  $1.5\text{V}$ .

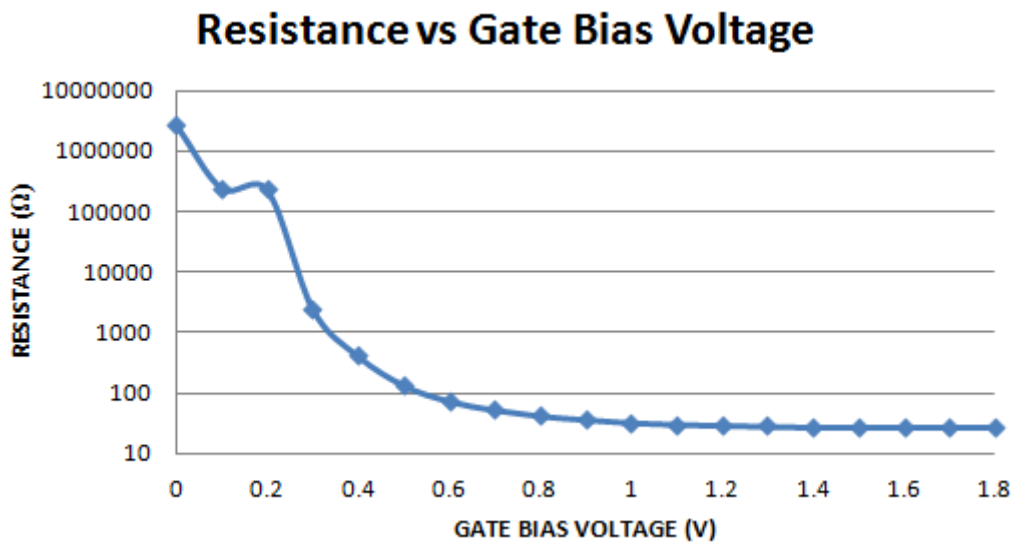


**Figure 9: Variation of Nmos On-Resistance with change in Gate Voltage**

Figure 10 shows the variation of Nmos on-resistance with respect to change in the transistor width for a fixed length of  $60\text{nm}$  and a fixed gate voltage of  $1.2\text{V}$ . We can see that as the width of the transistor is increased the resistance decreases. From this curve

we know the transistor on-resistances for different widths of the transistor and hence the width of the transistor switch can be set appropriately.

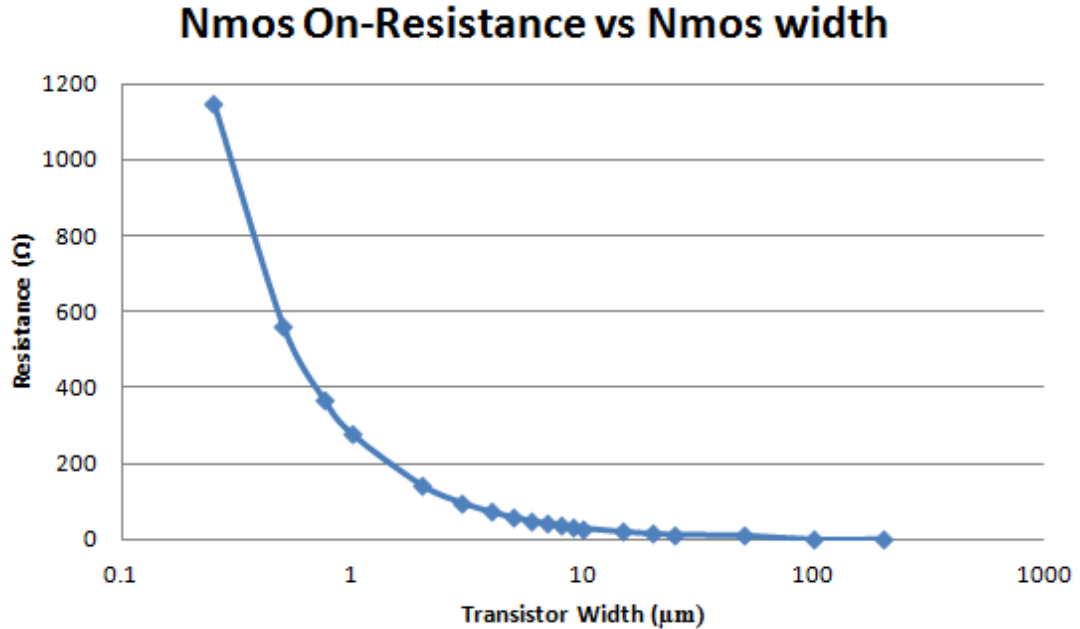


**Figure 10: Variation of Nmos On-Resistance with change in Transistor width**

TSMC NMOS MODEL	TRANSISTOR SIZE	NMOS RESISTANCE	RESISTOR VALUE
nch_mac 'M5'	L=130nm W=4um	117.3 Ω	R5 = 60.97 Ω
nch_mac 'M4'	L=60nm W=1.5um	176.5 Ω	R4 = 381.2 Ω
nch_mac 'M3'	L=60nm W=1.5um	176.5 Ω	R3 = 1KΩ
nch_mac 'M2'	L=60nm W=1.5um	176.5 Ω	R2 = 3KΩ
nch_mac 'M1'	L=60nm W=1.5um	176.5 Ω	R1 = 4.45KΩ

**TABLE 4: Transistor sizes, Transistor on-resistance and Resistor Values**

Table 4 gives the 5 NMOS transistor models, their sizes and corresponding on-resistance values. It also gives the compensated resistance values of the resistors that

form the resistor bank. Here 'nch\_mac' is a standard threshold voltage NMOS transistor available in the 65nm TSMC library. The corresponding resistance values of the 5 transistors are calculated and the resistance values of the resistors connected to these transistors is reduced by that amount so that the effective resistance remains the same. The first transistor is sized bigger to reduce the resistance of the transistor. All the other transistors are sized the same.

### **6.2.3 Use of Varactors for tuning**

The Roofing filter we are designing is a continuously tunable filter. In order to achieve this we have varactors at the heart of the design. Hence it is important to understand the working of the varactors. The varactors that we will be using are N-channel MOSFET based varactors.

MOSFET based varactors are implemented using a NMOS or PMOS transistor in which the drain, source and bulk are all connected together to form one terminal and the gate forms the other terminal. The MOS varactors are generally based on inversion mode MOSFETs or accumulation mode MOSFETs. The inversion mode MOSFETs have a high capacitance when a positive voltage is applied to the gate. This pulls the electrons closer to the gate forming a channel and forming an inversion region. Accumulation mode MOSFET varactors on the other hand have an  $n^+$  diffusion in an n-well rather than in a p-type region. The capacitance is high when a positive voltage is applied to the gate as this attracts the electrons forming an accumulation region. The accumulation mode varactors offer better performance because of lesser parasitic capacitances involved.



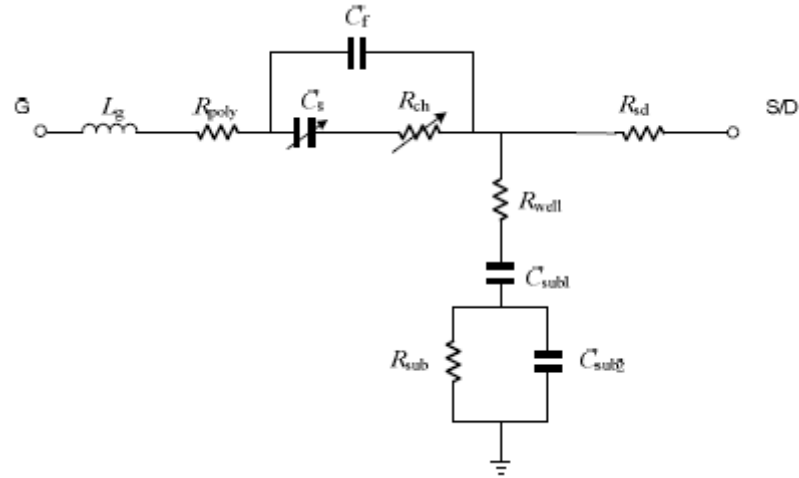


**Figure 11: Equivalent circuit model of accumulation-mode MOS varactor [32]**

The equivalent circuit model of an accumulation-mode MOS varactor is shown in figure 11. From the gate side  $L_g$  and  $R_{poly}$  represent the parasitic inductance and resistance of the gate.  $C_s$  refers to the gate oxide capacitance and the depletion region capacitance of the silicon layer under the gate oxide. This is the variable capacitance of the MOS varactor.  $C_f$  represents the fringing capacitance mainly due to the sidewall of the gate.  $R_{ch}$  represents the channel resistance and  $R_{well}$  represents the resistance of the n-well.  $C_{sub1}$  represents the depletion capacitance between the n-well and the p-substrate. The parallel combination of  $R_{sub}$  and  $C_{sub2}$  represents the losses in the silicon substrate that occur at high frequency [32].

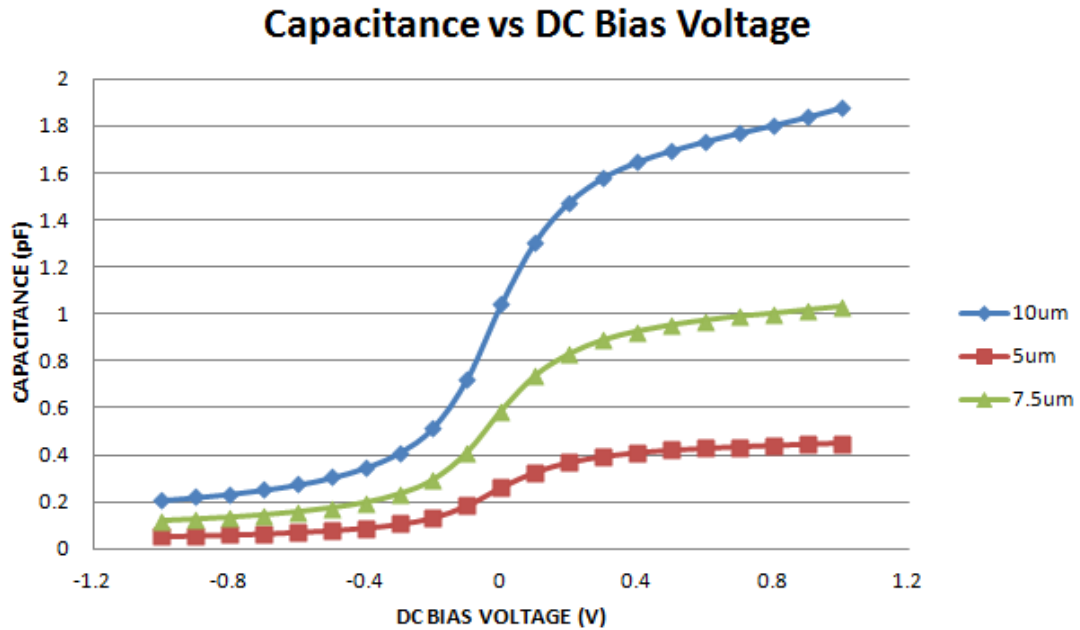


**Figure 12: Variation of TSMC varactor capacitance with DC bias voltage**

Figure 12 shows the variation of the TSMC varactor capacitance with DC bias voltage applied across the varactor. The varactor we have chosen is an nmoscap varactor, which is working in the accumulation mode. The DC voltage across the varactor is varied from -1V to 1V and the capacitance is measured. For measuring the capacitance we make use of a simple RC network that works as a low-pass filter as shown in figure 13.

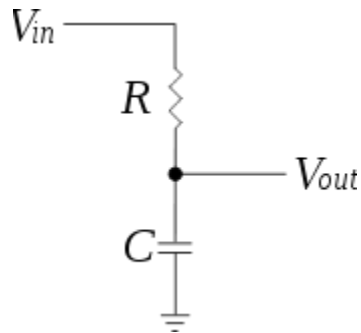


**Figure 13: Simple RC network to measure the capacitance of the varactor**

We plot the magnitude response of the low-pass filter and from the cut-off frequency we obtain the capacitance as:

$$C = \frac{1}{2\pi f_c R}$$

The capacitances vs. DC bias voltage curves are plotted for three different varactor sizes, 10 $\mu\text{m}$ , 7.5 $\mu\text{m}$  and 5 $\mu\text{m}$ . Each of the varactor is working in the accumulation mode and has a same pattern of variation of capacitance with respect to DC bias voltage. As the voltage across the gate is high and far beyond the flat-band voltage, the silicon surface accumulates electrons from the drain/source regions. The capacitance observed is the oxide capacitance. As the gate voltage is decreased the number of electrons accumulated decreases and at the flat-band voltage the silicon surface becomes completely charge free. When the applied voltage falls below the flat-band voltage the surface undergoes depletion. The capacitance varies from a maximum value at accumulation to a minimum value at depletion. From the curves in figure 12 we observe that as we increase the varactor size the range of the varactor capacitance increases. The 5 $\mu\text{m}$  varactor has a capacitance range of 0.396pF, the 7.5 $\mu\text{m}$  varactor has a range of 0.91pF whereas the 10 $\mu\text{m}$  varactor has a capacitance range of 1.667 pF.

But as the size of the varactors grows bigger the parasitic resistances and capacitance associated with it also grow. Hence it is preferable to use multiple varactors of smaller size that can be controlled by switches. For this purpose we use PMOS transistor switches.

In the design of the Roofing filter we have used 5 varactors of different sizes connected in parallel to achieve a tuning range of 2GHz i.e. from 0.7GHz to 2.7GHz. The number of varactors was fixed at 5, as this was the least number of varactors that were required to achieve the frequency range and also meet the bandwidth requirements. Each of these varactors is connected to a PMOS transistor and hence can be connected or

disconnected from the circuit by turning the transistor on and off. The capacitance of the varactor depends on the voltage drop across it. One end of the varactor is maintained at a constant potential of 1.2V. The DC voltage at the other end of the varactor is varied. This DC voltage at the other end is supplied through a high value resistor. The high value resistor is used in order to provide a good isolation from noise. The high value resistor does not have a voltage drop across it, as there is no DC current flowing through the resistor. We also use a fixed capacitor in the circuit as a DC block so that we have complete control over the DC voltage that appears across the varactor.

<b>PMOS MODEL</b>	<b>TRANSISTOR SIZE</b>	<b>VARACTOR MODEL</b>	<b>VARACTOR SIZE</b>	<b>RESISTOR VALUE</b>	<b>DC BLOCK CAPACITOR VALUE</b>
pmos_rf 'M6'	W=64um L=60nm	nmoscap_25 'C7'	W=23.2um L=23.2um	'R8'=50K	'C1'= 10pF
pmos_rf 'M7'	W=40um L=60nm	nmoscap_25 'C8'	W=11.8um L=11.8um	'R9'=50K	'C3'= 10pF
pmos_rf 'M8'	W=28.8um L=60nm	nmoscap_25 'C9'	W=5.4um L=5.4um	'R10'=50K	'C4'= 10pF
pmos_rf 'M9'	W=16.8um L=60nm	nmoscap_25 'C10'	W=2.9um L=2.9um	'R11'=50K	'C5'= 10pF
pmos_rf 'M10'	W=6um L=60nm	nmoscap_25 'C11'	W=1.5um L=1.5um	'R12'=50K	'C6'= 10pF

**TABLE 5: Transistor Sizes, Varactors, Resistor and Capacitor Values**

Table 5 gives the various device parameters used in the Roofing filter design. The PMOS transistor model used is 'pmos\_rf', an RF transistor that is available in TSMC

65nm library. The PMOS transistors are sized according to the bandwidth and range requirements and it generally is a tradeoff between the two. As the size of the transistor is increased the resistance of the transistor decreases and hence the bandwidth reduces but the range that can be achieved is limited. This is the reason the transistors are sized in a decreasing order. The varactors are sized in a decreasing order with the first varactor having largest size and hence the highest range and the last varactor has the least size and the smallest range. The capacitance values obtained from MATLAB for a particular inductance value (19nH here) are used as reference to size the varactors and achieve the required capacitance values. The varactors are turned on and off by the PMOS transistors. This allows us to combine the varactors in parallel to obtain higher or lower capacitance values. The varactors are sized by keeping the capacitance values obtained from MATLAB as reference. The sizing of the varactors also depends on the tuning range of the Roofing filter that has to be achieved.

#### **6.2.4 Roofing Filter Termination, Bias Voltages and Control Voltages**

For maximum power transfer, the load impedance and the source impedance should be equal. Here we design the circuit for a  $50\Omega$  load and source termination. Hence in reference to Figure 8 we have resistor  $R7=50\Omega$  which is the source resistance and the resistor  $R6$  is set to  $45\Omega$  so that the effective input impedance of the circuit is as close as possible to  $50\Omega$ . We also have a capacitor 'C2' at the input as DC block.

The inductor is connected to a constant DC voltage source of  $V3=900\text{mV}$ . This is a constant DC bias voltage.

We have two control voltages in the circuit. One voltage is  $V_C$ , which is the voltage at one end of the varactor. This voltage is used to change the center frequency of the

Roofing filter. VC is varied from 200mV to 1.2V, which changes the capacitance of the varactor and hence the center frequency of the roofing filter is changed. The other control voltage in the circuit is VB. This is another bias voltage in the circuit. This is represented by the voltage source 'V1' in the circuit diagram. This voltage is varied from 200mV to a maximum value of 835mV. The input is represented by the voltage source 'V2'.

## CHAPTER 7

### EXPERIMENTAL RESULTS FOR THE ROOFING FILTER PRE-LAYOUT SIMULATION

In order to verify the correctness of the design and also measure the performance of the Roofing filter various simulations are first run on the schematic. Running the simulations on the schematic helps us identify the sources that are limiting the performance of the filter. While we designed the filter in MATLAB we did not have a lot of constraints on the design of the filter. In the actual design of the design there are constraints on the Bandwidth of the filter, the voltages that can be used and sizing of the devices. These constraints have to be satisfied while ensuring that the best performance of the filter is being achieved.

#### 7.1 Corner Simulations

Various simulations have been run to test the performance of the Roofing filter. Each of these simulations has been done for the three process corners, TT (Typical-Typical) corner, SS (Slow-Slow) corner and FF (Fast-Fast) corner. A process corner refers to the variation of fabrication parameters in the integrated circuit design. These corners represent the extreme variations of these parameters i.e. the SS and FF corners typically represent +/- 3-sigma variation of the parameters from their values in the TT corner. At these corners the circuit may run faster or slower than the TT corner but if the circuit does not function at all then it means that the design margins considered are inadequate. While performing the corner simulations we have considered that all the devices present in the roofing filter circuit are in that particular corner, which might not be always the case in reality.

##### 7.1.1 Frequency Response

The frequency response of a filter is an important indicator of the performance of the filter. The frequency response is the quantitative measure of the output of a system in response to an input. Here we plot the magnitude response of the roofing filter in all the three corners. In order to show that the filter can indeed attain a frequency range of 2GHz i.e. from 0.7GHz to 2.7GHz, we plot the magnitude response for the same 31 frequencies as before. In order to set the roofing filter to a particular center frequency we do the following:

- I. We have to set the inductor value. As this value is already fixed we proceed to set the capacitance values. We set the capacitance to the required value in order to set the center frequency of the filter. We have 5 varactors, which are connected to 5 PMOS transistor switches. Each of these switches can be turned on and off to connect or disconnect the varactors. The switches are set according to the required capacitance value. For a low frequency a high capacitance value is required and vice versa. The highest capacitance value is obtained by turning all the varactors on, which adds the capacitances in parallel. This is done for the lowest frequency of operation. As the frequency increases the varactors are turned off to reduce the effective capacitance.
- II. After the varactor switch setting is decided, we have one or more varactors that are turned on. These varactors have a range of capacitance that they can operate at. In order to set the center frequency to one particular value we have to set the voltage 'VC' across the varactors to get the appropriate capacitance value. We have designed the roofing filter such that VC is a common voltage for all the varactors. The varactor bias voltage VC is varied from 1.2V to 0.2V. Increasing



‘VC’ increases the voltage across the varactor, which increases the varactor capacitance, which shifts the center frequency to a lower value. Decreasing ‘VC’ decreases the voltage across the varactor and the capacitance reduces and hence the frequency shifts to a higher value.

III. The roofing filter has two main constraints, insertion loss and bandwidth. The insertion loss of the roofing filter should be as low as possible and since the roofing filter will be used to eliminate large out-of-band signals, the lesser the bandwidth of the filter the better. But since the frequency of operation of the filter is very high it becomes increasingly difficult to maintain a very low bandwidth. We use the resistor bank and the bias voltage VB to set the bandwidth and insertion loss of the filter to the required values. The resistor bank has 5 switches, which can be turned on and off to get 31 different resistance values. By keeping the resistance values from MATLAB as reference we obtain the resistor switch settings. The bias voltage VB is varied from 200mV to a maximum of 835mV.

The following tables and figures give the switch settings and voltage settings for the magnitude response of the roofing filter at 31 center frequencies in all the 3 corners.

<b>CENTER FREQUENCY (GHz)</b>	<b>RESISTOR SWITCH SETTING</b>	<b>VARACTOR SWITCH SETTING</b>	<b>VC (V)</b>	<b>VB (V)</b>
0.7000	11111	00000	1.14	725m
0.7660	11111	00000	906m	738.5m
0.8330	11111	00000	710m	750.5m

0.9000	11111	00000	535m	760m
0.9670	11111	00000	360m	768.5m
1.0300	11111	01000	460m	764m
1.1000	11111	01000	280m	772m
1.1670	11111	01100	220m	774m
1.2330	11111	10000	1.03	779.5m
1.3000	11111	10000	880m	785.5m
1.3660	11111	10000	740m	791.5m
1.4330	11111	10000	600m	797m
1.5000	11101	10000	460m	795.5m
1.5660	11100	10000	300m	793m
1.6330	11100	10100	430m	791m
1.7000	11100	10100	270m	796m
1.7660	11000	10110	280m	787m
1.8330	11000	11000	1.17	795m
1.9000	10000	11000	1.02	785m
1.9660	10000	11000	850m	789.5m
2.0330	10000	11000	665m	794m
2.1000	10000	11000	440m	798.5m
2.1660	01100	11010	685m	793m
2.2330	01100	11010	470m	799m
2.3000	01000	11011	430m	778.5m
2.3670	01000	11100	1.02	776.5m
2.4330	01000	11100	770m	779.5m
2.5000	01000	11100	260m	786m
2.5660	01000	11101	450m	795.5m
2.6300	01000	11110	1.1	791m

2.7000	01000	11110	650m	798.5m
--------	-------	-------	------	--------

**TABLE 6: Center frequencies, switch settings and Bias voltage values in TT corner**

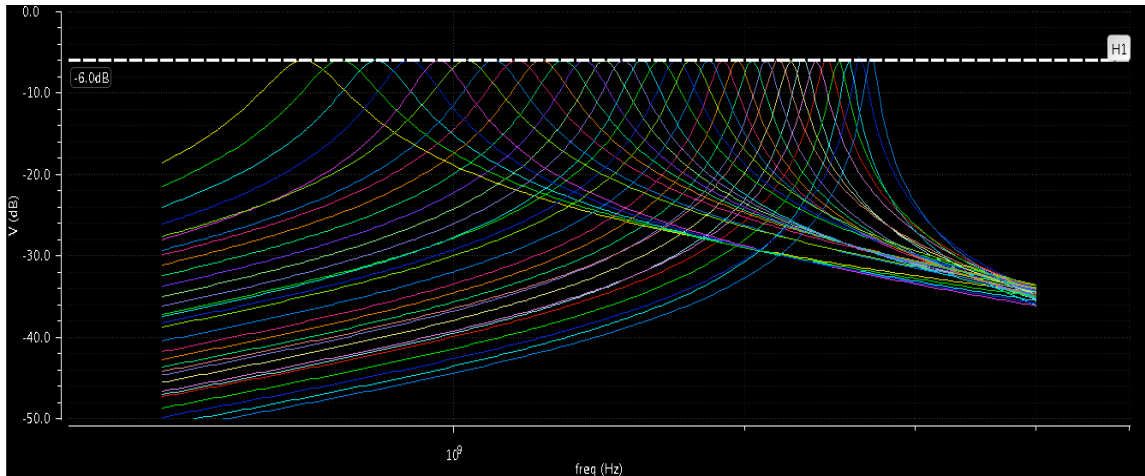


**Figure 14: Magnitude response of the Roofing filter schematic in TT corner**

CENTER FREQUENCY	RESISTOR SWITCH SETTING	VARACTOR SWITCH SETTING	VC (V)	VB (V)
0.7000	11111	00000	1.2	637m
0.7660	11111	00000	950m	654m
0.8330	11111	00000	755m	667.5m
0.9000	11111	00000	590m	679m
0.9670	11111	00000	425m	689m
1.0300	11111	00000	235m	698m
1.1000	11111	01000	350m	692.5m
1.1670	11111	01100	290m	694.5m
1.2330	11110	10000	1.09	695.5m
1.3000	11110	10000	930m	703m
1.3660	11000	10000	790m	695m

1.4330	10000	10000	658m	690.5m
1.5000	10000	10000	510m	700m
1.5660	10000	10000	360m	708m
1.6330	10000	10100	490m	703m
1.7000	01101	10100	340m	690m
1.7660	01010	10110	340m	673.5m
1.8330	01010	10111	235m	680.5m
1.9000	01000	11000	1.06	658.5m
1.9660	01000	11000	900m	664.5m
2.0330	00100	11000	705m	669.5m
2.1000	00100	11000	490m	675m
2.1660	00100	11000	210m	679.5m
2.2330	00100	11010	520m	682.5m
2.3000	00100	11011	480m	688m
2.3670	00100	11100	1.05	686.5m
2.4330	00100	11100	790m	692m
2.5000	00100	11100	260m	698.5m
2.5660	00010	11101	350m	708.5m
2.6300	00011	11110	1.11	725m
2.7000	00001	11110	500m	709.5m

**TABLE 7: Center frequencies, switch settings and Bias voltage values in SS corner**

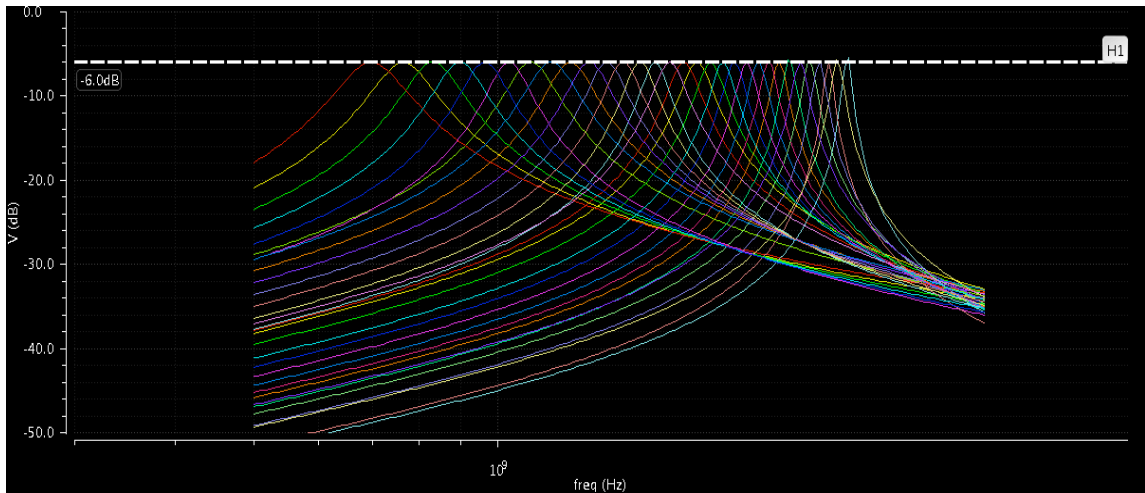


**Figure 15: Magnitude response of the Roofing filter schematic in SS corner**

CENTER FREQUENCY	RESISTOR SWITCH SETTING	VARACTOR SWITCH SETTING	VC (V)	VB (V)
0.7000	11111	00000	1.11	793m
0.7660	11100	00000	865m	797m
0.8330	11010	00000	670m	798.5m
0.9000	11000	00000	490m	800m
0.9670	11000	00000	300m	809m
1.0300	11000	01000	405m	805.5m
1.1000	10110	01000	210m	820m
1.1670	10110	01111	220m	823m
1.2330	10100	10000	970m	818m
1.3000	10100	10000	830m	824.5m
1.3660	10010	10000	700m	819m
1.4330	10001	10000	550m	820.5m
1.5000	10000	10000	400m	815.5m
1.5660	10000	10000	230m	821m
1.6330	10000	10100	375m	820m

1.7000	01000	10100	200m	819m
1.7660	01000	10110	200m	823m
1.8330	00100	11000	1.14	820m
1.9000	00100	11000	980m	825m
1.9660	00100	11000	810m	830m
2.0330	00100	11000	635m	832m
2.1000	00100	11000	410m	835m
2.1660	00010	11010	640m	800m
2.2330	00010	11010	440m	815m
2.3000	00010	11011	400m	825m
2.3670	00010	11100	1.01	824.5m
2.4330	00010	11100	770m	830m
2.5000	00010	11100	275m	835m
2.5660	00001	11101	450m	831m
2.6300	00001	11110	1.1	820m
2.7000	00001	11110	725m	835m

**TABLE 8: Center frequencies, switch settings and Bias voltage values in FF corner**

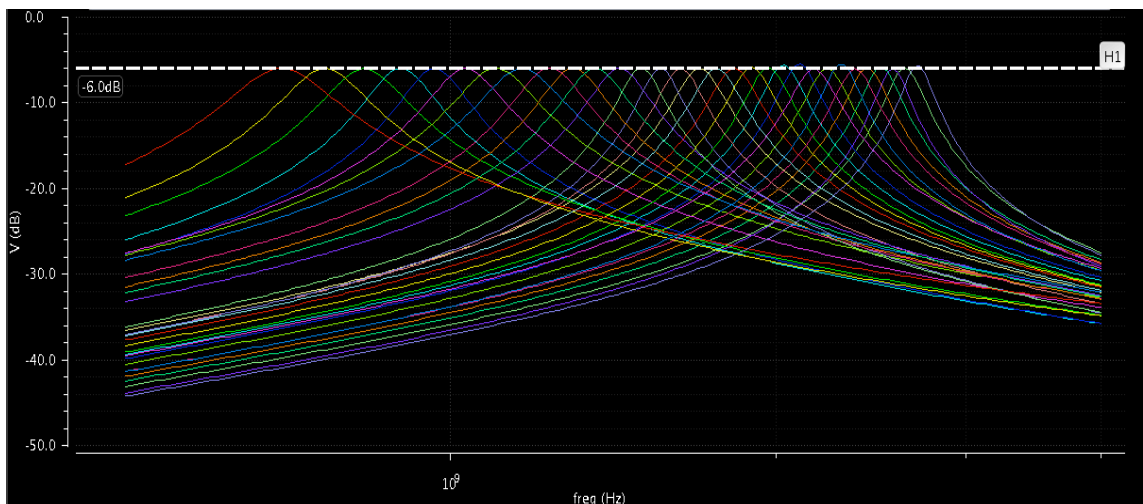


**Figure 16: Magnitude response of the Roofing filter schematic in FF corner**

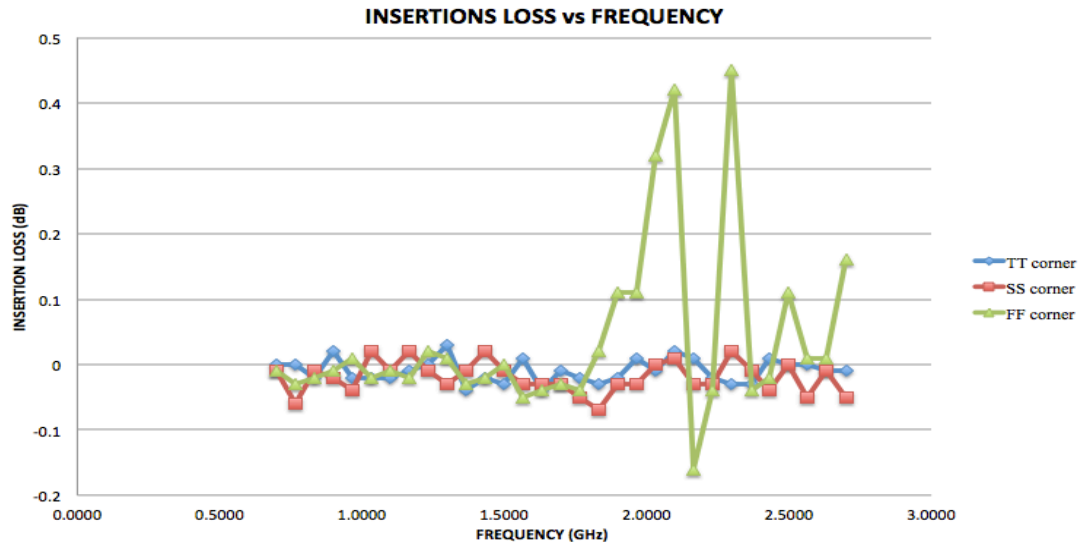
Tables 6, 7 and 8 show the center frequencies, their corresponding switch settings for the resistor bank, varactor switch settings and bias voltages for the TT corner, SS corner and FF corner respectively. Using these values the magnitude response of the roofing filter is plotted.

Figure 14, Figure 15 and Figure 16 show the magnitude response of the roofing filter in TT corner, SS corner and FF corner respectively for 31 center frequencies. We have plotted the Roofing filter magnitude response for 31 center frequencies as we have done before. This is done in order to show that the Roofing filter can indeed attain the desired frequency range of 2GHz. But using the varactors the center frequency of the Roofing filter can be set to any frequency in the range of 0.7GHz to 2.7GHz. In the figures we have a horizontal line at the -6dB mark to show the insertion loss of the filter. It has to be noted that the 6dB loss is not the insertion loss of the filter but it comes from the 50Ω source impedance.

### **7.1.2 Insertion loss and Bandwidth**

Figure 17 shows the variation of insertion loss of the roofing filter with center frequency in the TT corner, SS corner and FF corner. From the figure it can be seen that very low insertion loss was obtained in all the three corners over the entire frequency range of 2GHz. The maximum variation of insertion loss is observed in the FF corner. The total variation in the FF corner is around 0.61 dB i.e. variation from the maximum value to the minimum value. We observe some gain in the filter because at the input of the roofing filter we have a resistor bank with NMOS switches, which act as a common gate amplifier to provide some gain in the circuit. This effect is enhanced in the FF corner compared to the other corners. Also the resistance values of the resistors in the resistance

bank are reduced in the FF corner. In the SS corner and TT corner it can be observed that the maximum variation is of the order of  $\pm 0.05\text{dB}$ . But it has to be noted that the insertion loss is well within the accepted variation of  $\pm 0.5\text{dB}$  in all the three corners.



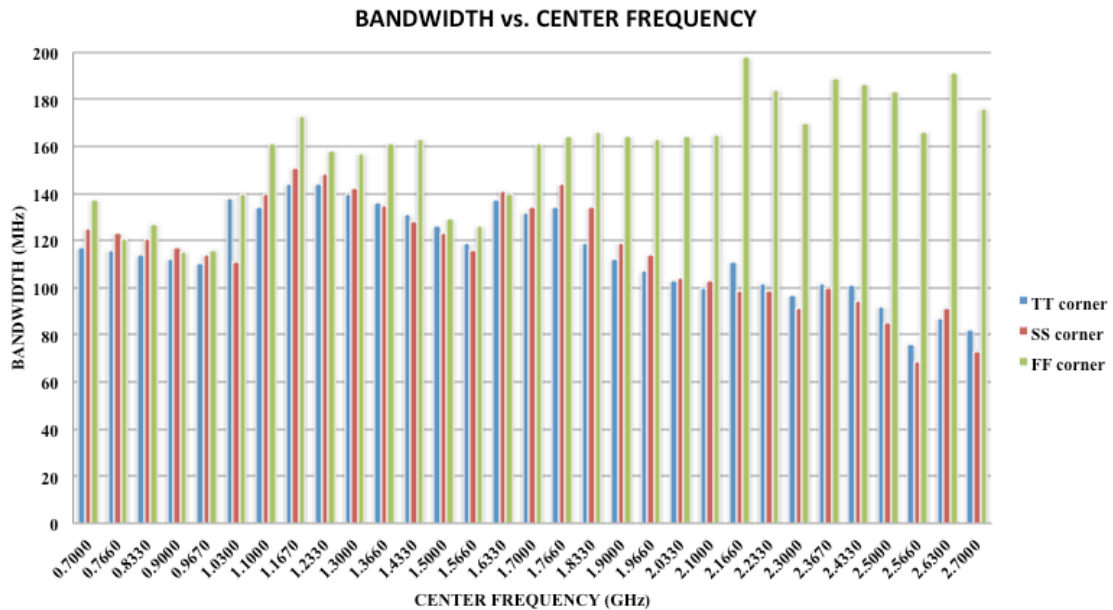
**Figure 17: Insertion loss of the roofing filter vs. Frequency**

Figure 18 shows the variation of the Roofing filter bandwidth with center frequency for all the three corners. It can be observed from the figure that the bandwidth of the Roofing filter is under 200MHz over the entire frequency range and for all the three corners. While in all the three corners we observe a similar trend in bandwidth variation, FF corner has higher bandwidths than the TT and SS corner. When we designed the Roofing filter, we designed the resistance and capacitance values from MATLAB. This was done so for the ideal case, which is closely represented by the TT corner. When we simulate in the FF and SS corners the parameters of the devices change but we do not change the device values. Hence we observe deviations from the expected results. One of the factors contributing to high bandwidth in the FF corner is the varactor. In the FF corner the varactors have higher capacitance values and lower Q-factors. This low Q-factor results in the increase in the bandwidth of the filter. The resistances of the



resistors in the resistor bank are lower in the FF corner, which is also a contributing factor for the increase in bandwidth.

In the TT corner the fractional bandwidth i.e. the ratio of bandwidth to center frequency varies from a maximum value of 16.71% at 0.7GHz to a minimum value of 2.97% at 2.566GHz. In the SS corner it varies from a maximum value of 17.86% at 0.7GHz to 2.71% at 2.7GHz. In the FF corner the fractional bandwidth has a maximum value of 19.57% at 0.7GHz and a minimum value of 6.47% at 2.566 GHz.



**Figure 18: Bandwidth of the roofing filter vs. Center Frequency**

### 7.1.3 Parametric Analysis

Parametric analysis refers to the analysis where one parameter of the circuit is varied and the performance of the circuit is measured. One of the most important parameters that can change the performance of a system is the temperature of the system. Here we have tested the Roofing filter circuit under three operating temperatures, a minimum temperature of 0°C, nominal temperature of 27°C and a maximum temperature

of 85°C. We have run these simulations for all the three corners to measure the insertion loss and bandwidth of the filter.

As it can be seen from the figures 19, 20 and 21 we have taken the insertion loss at 27°C as the reference value and we have compared the variation of insertion loss at 0°C and 85°C. In the TT and SS corner the insertion loss decreases with increase in temperature. We can observe gain in the filter at 85°C. This can be attributed to the fact that at the input of the filter we have NMOS switches, which act as a common gate amplifier providing gain in the circuit. At higher temperatures the drain currents of the transistor are lower and hence this effect is enhanced at higher temperatures. We observe up to 3dB of gain in the TT corner and almost 3.4dB of gain in the SS corner at 85°C. In the FF corner we observe lesser variation of insertion loss compared to the SS and TT corners except at a few points where we see a lot of variation. The effect of the NMOS transistors acting as common gate amplifiers is negated to some extent in the FF corner. This is because in the FF corner the transistors have lower threshold voltages, shorter channel lengths etc. and as a result the drain currents are high. As the temperature of the circuit is decreased to 0°C the insertion loss increases in both the TT and SS corners whereas in the FF corner it first increases and then decreases. This can be attributed to the fact that the drain currents of the NMOS transistors increase at lower temperatures which increases the insertion loss. This shows that the insertion loss of the Roofing filter is affected by temperature changes. The temperature changes also result in minor shifts in the center frequency. This shift in center frequency is due to the fact that the capacitance of the varactor changes with change in temperature. These effects can be reduced to some extent by adjusting the bias voltages of the Roofing filter.

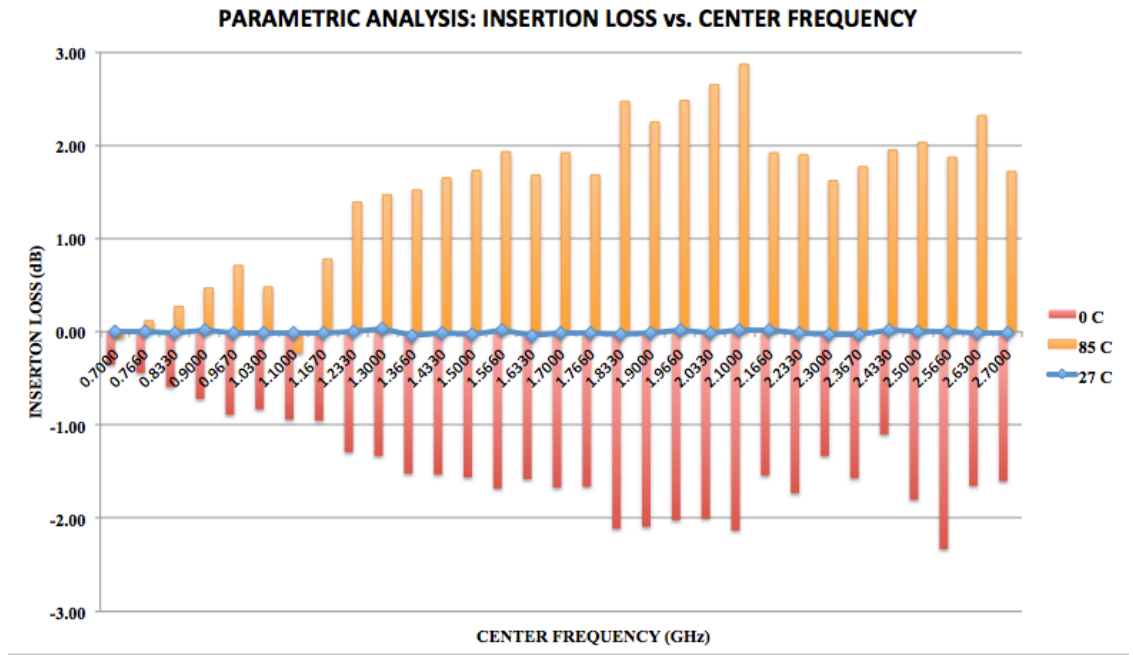


Figure 19: Parametric Analysis: Insertion loss vs. Center Frequency in TT corner

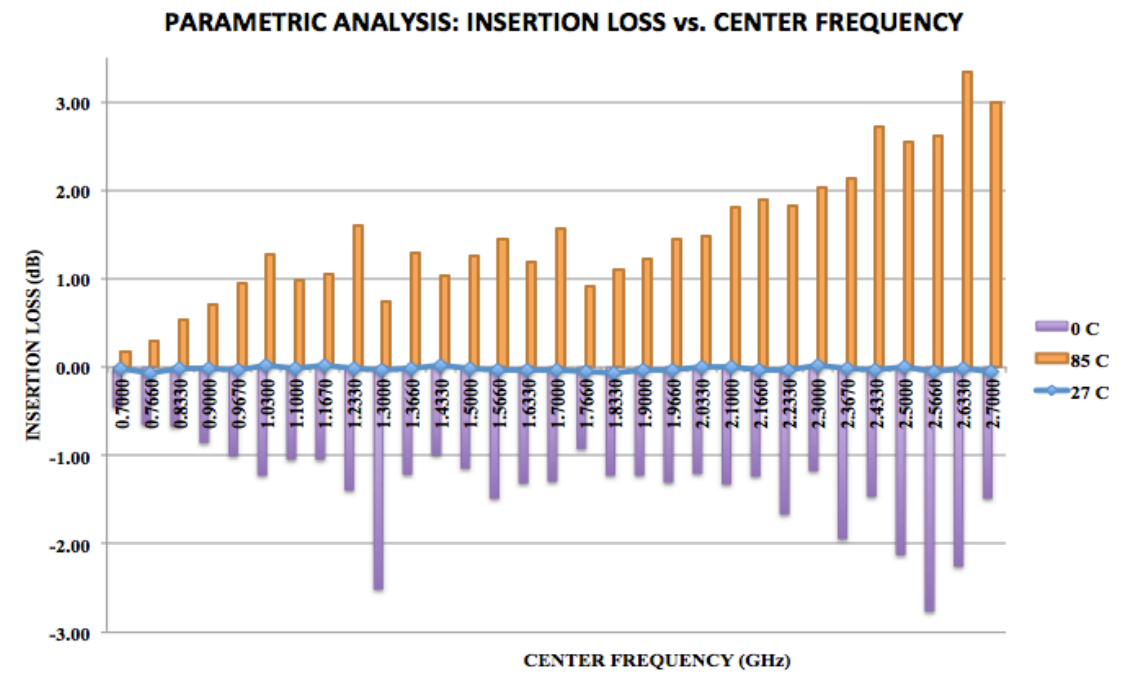
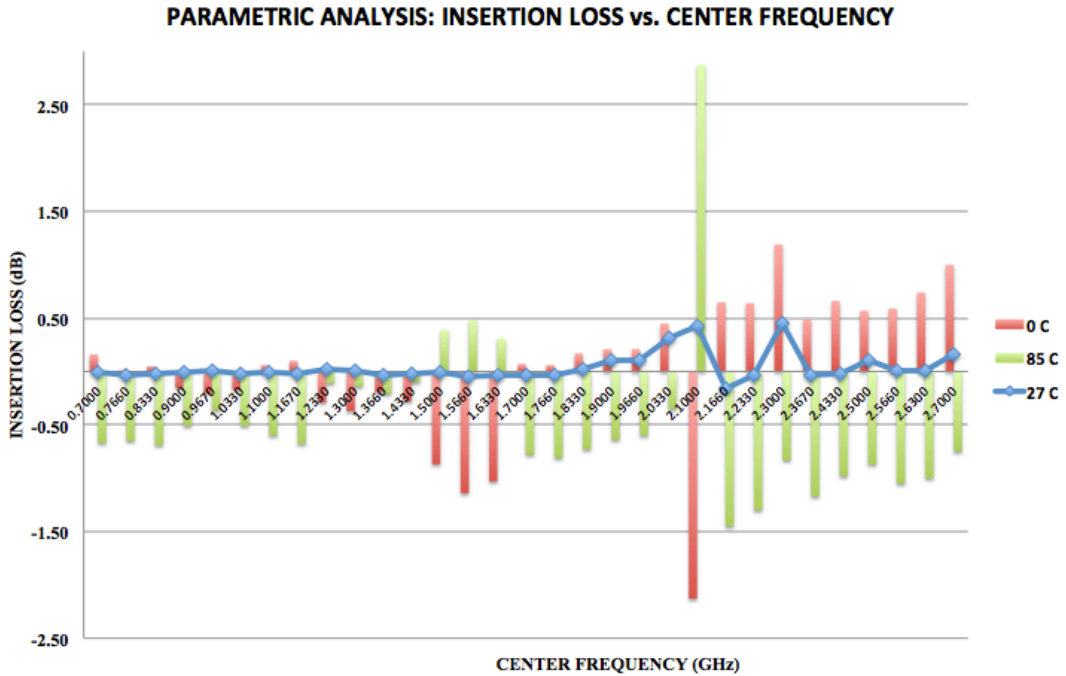


Figure 20: Parametric Analysis: Insertion loss vs. Center Frequency in SS corner



**Figure 21: Parametric Analysis: Insertion loss vs. Center Frequency in FF corner**

Figure 22, Figure 23 and Figure 24 gives the variation of the bandwidth of the Roofing filter with center frequency for TT corner, SS corner and FF corner respectively for three temperatures 0°C, 27°C and 85°C. The general inference that can be drawn from observing all the three corners is that the bandwidth of the Roofing filter increases with increase in temperature i.e. it is highest at 85°C and lowest at 0°C. A lot of factors contribute towards this increase in bandwidth. The increase in temperature increases the parasitic resistance values of the varactors and transistors. This increase in resistance increases the bandwidth of the filter. At TT and SS corners the bandwidth of the filter is less than 180MHz at 85°C. In the FF corner there are a few points at which the bandwidth goes beyond 200MHz. One thing has to be noted is that the even though the Roofing filter is subject to extreme operating conditions in these simulation, on an average the performance of the Roofing filter has been good. The other thing to be noted is that the switch settings and voltage settings were not changed for the Roofing filter as

the temperature was increased or decreased i.e. it was maintained the same as it was for the normal temperature of 27°C. Hence these variations can be reduced up to some extent by changing the switch settings and voltage settings and by adjusting the bias voltages of the Roofing filter.

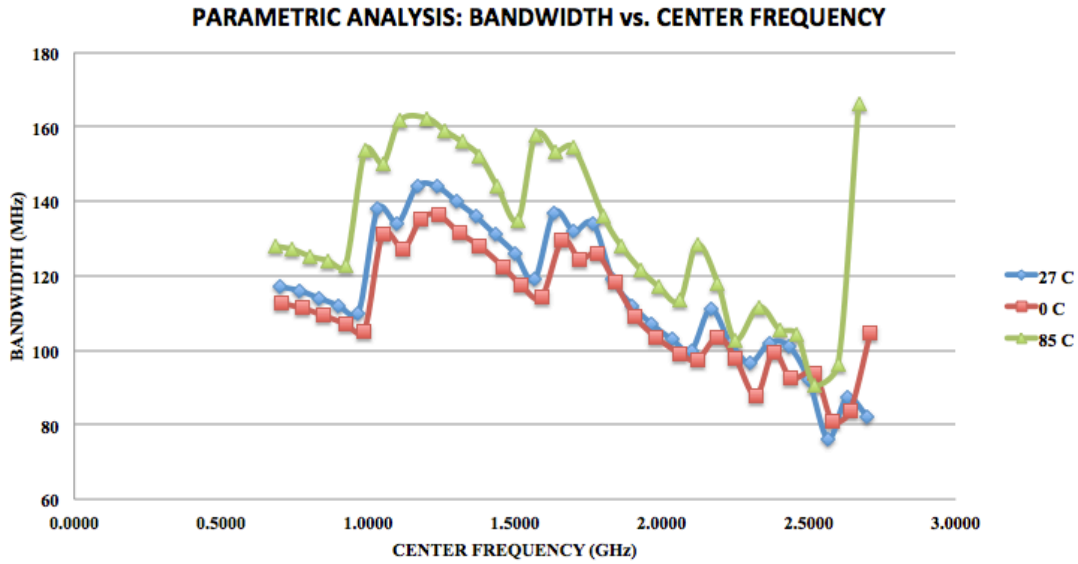


Figure 22: Parametric Analysis: Bandwidth vs. Center Frequency in TT corner

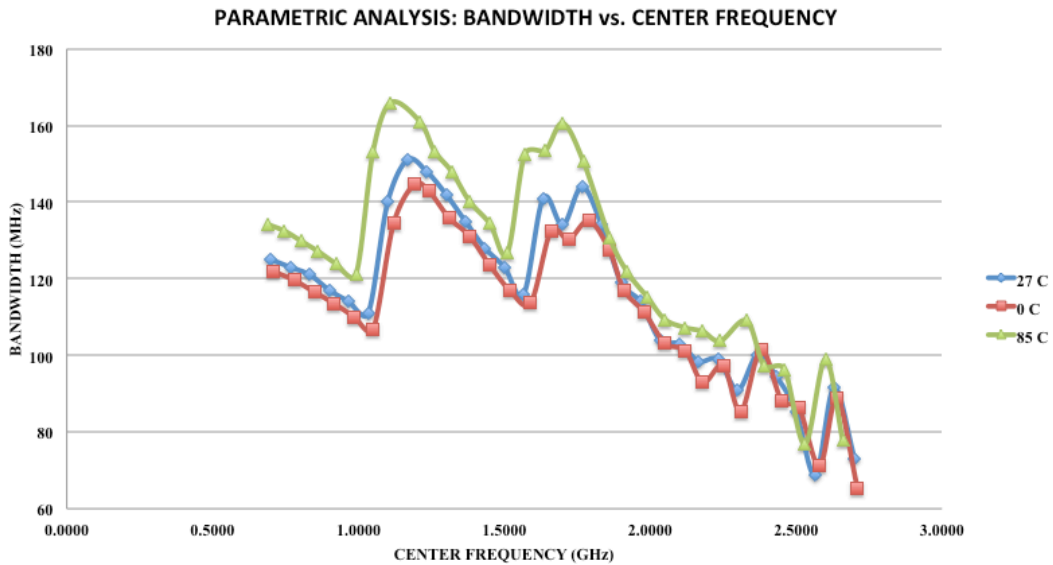
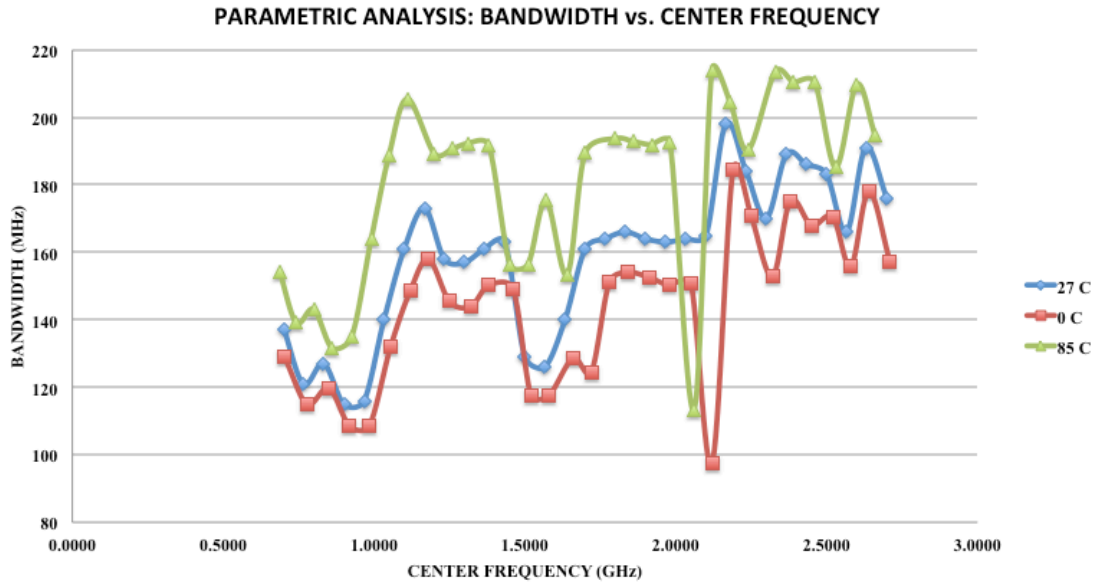


Figure 23: Parametric Analysis: Bandwidth vs. Center Frequency in SS corner



**Figure 24: Parametric Analysis: Bandwidth vs. Center Frequency in FF corner**

#### 7.1.4 Monte Carlo Simulations

During the manufacturing process of an integrated circuit there are a lot of variations that can occur from device to device, die to die and wafer to wafer. These variations or mismatches in device parameters can cause changes in the functionality of the circuit. These variations are random in nature and hence the response of the circuit to these variations cannot be predicted with certainty. For this reason statistical simulations like Monte-Carlo simulations are used. In Monte-Carlo simulation the parameters of each device is varied randomly and the combined effect of this on the performance of the entire circuit is analyzed. This technique helps us to understand the robustness of our design and also the response of the circuit to mismatches that occur due to process variation. The figure below shows the Monte-Carlo simulation output for all the three corners. Here we have run the Monte-Carlo simulation for mismatch and not for process variation. By running the Monte-Carlo simulation in all the three corners we are testing the circuit for the worst case mismatches in the worst process corner. These kinds of

variations may never occur but these simulations are run in order to test the robustness of the circuit in the worst possible scenarios. The number of Monte-Carlo runs was fixed at 50. For each of the runs the bandwidth of the roofing filter was measured. The mean value and standard deviation of the bandwidths were taken. In the figure below we have plotted the standard deviation of the bandwidth versus the center frequency. From the results obtained from the Monte-Carlo simulations it was observed that the mean bandwidths that were obtained were in close agreement with the bandwidths obtained during normal simulations. From the figure we observe that the standard deviation in the TT and SS corners are less than 2MHz over the entire frequency range. This shows the robustness of the circuit to process variations in the TT and SS corner. In the FF corner, which is the worst corner the maximum standard deviation obtained is around 14MHz, which is quite good considering the high frequency of operation and bandwidth. This shows that the Roofing filter that we have designed is robust and can perform well even under parameter mismatch.

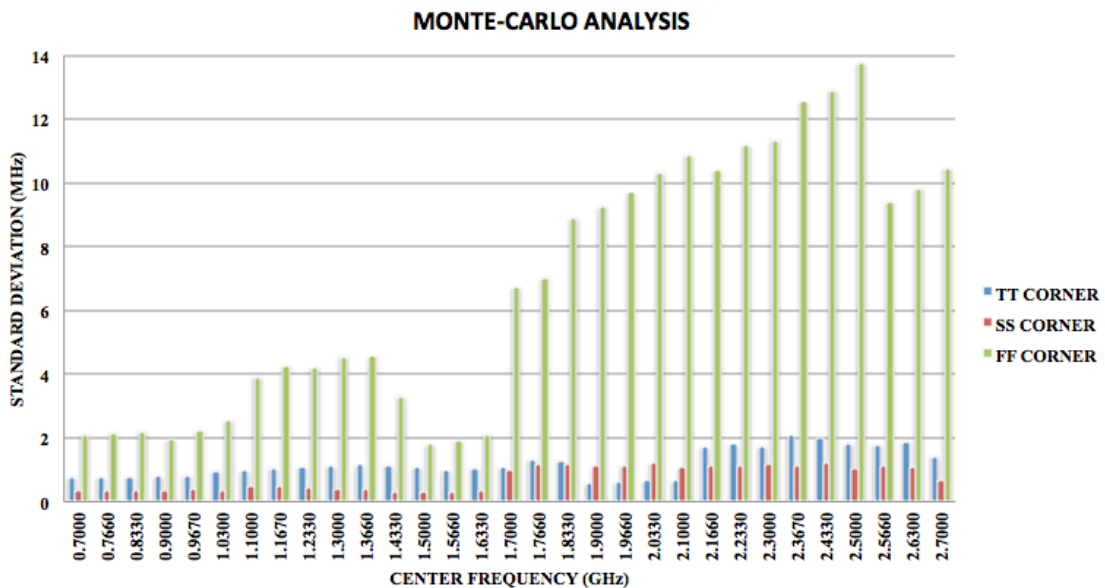


Figure 25: Monte-Carlo Simulations for device mismatch

### 7.1.5 Return Loss

Return loss is defined as the loss of signal power resulting from reflections caused due to impedance mismatch. It can also be defined as the effectiveness with which the power is delivered from the source to the load. This effectiveness depends on how well the source impedance matches the load impedance. The return loss is expressed in dB. The higher the value of return loss the better is the impedance matching between the load and the source and hence the loss of signal power is lesser.

Figure 26 shows the variation of return loss of the roofing filter with center frequency for all the three corners. From the figure it can be observed that the best performance in terms of return loss is observed in the SS corner where the return loss goes from around 19dB at 0.7GHz to around 25dB at 2.7GHz. In the FF corner the performance is not as good as the SS corner but the return loss values are more than 15dB and are fairly constant through out the frequency range. The performance in the TT corner is in between the SS and FF corners. The return loss increases from around 12.4dB at 0.7GHz to around 21.3 dB at 2.7GHz for the TT corner.



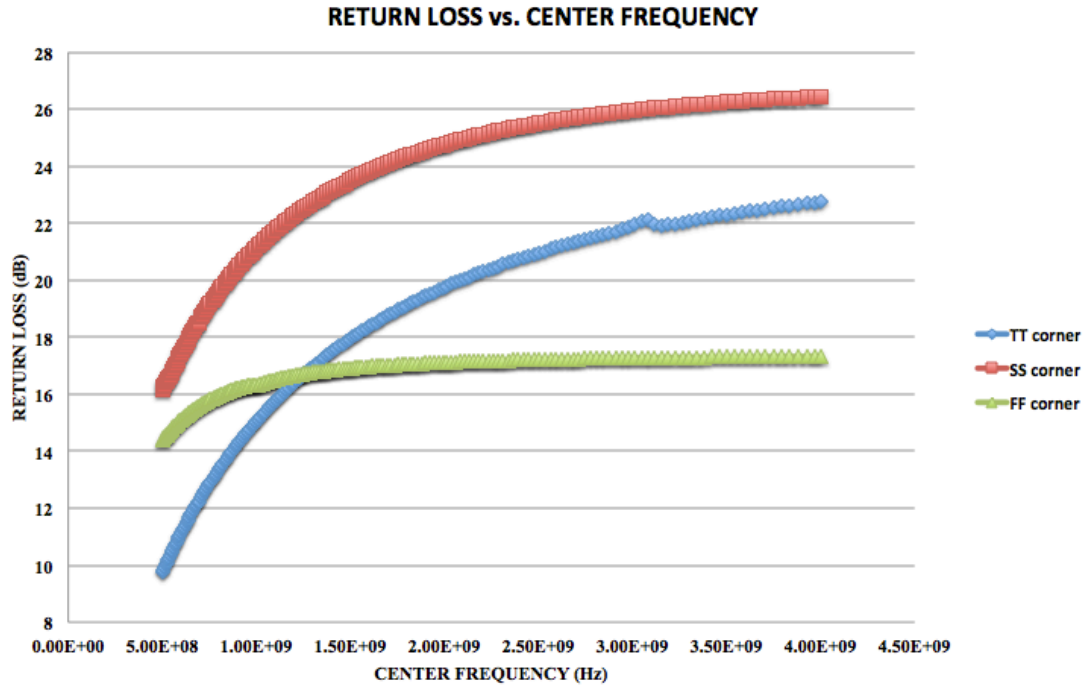


**Figure 26: Return Loss of Roofing Filter**

### 7.1.6 Roofing Filter Linearity

For an ideal system the ratio of the output power to input power is constant for all values of input power. In an actual system the output power increases linearly with increase in the input until such a point where the distortion product energy combines with the fundamental output and this combination is observed at the output. After this point the ratio of the output power and input power ceases to be a constant. At some value of the input signal level the output signal power becomes 1dB less than the output signal power of an ideal system. This point is known as the 1-dB compression point. Figure 27 shows the 1dB compression point analysis for the Roofing filter performed at 1GHz center frequency for TT and FF corner. From the figure it can be seen that we have plotted the graph as ratio of output voltage to input voltage in dB versus input voltage in dBmV. This is done because the output of the roofing filter will end up in a very high

resistance and it is not meaningful to calculate output power. Hence we do not plot an output power versus input power graph for 1dB compression analysis. From the analysis taking -0.15dB as reference point, we get the 1dB compression point at 1GHz center frequency for the TT corner as 56dBmV. For the FF corner taking 0.2dB as reference point we get 47dBmV as the 1dB compression point. In the SS corner at center frequency of 1GHz we see an expansion of up to 0.9 dB and then compression. The compression point analysis was also performed for a center frequency of 2GHz in all the three corners. Both expansion and compression was observed in the TT and SS corners. At the FF corner the compression point was found to be 49dBmV.

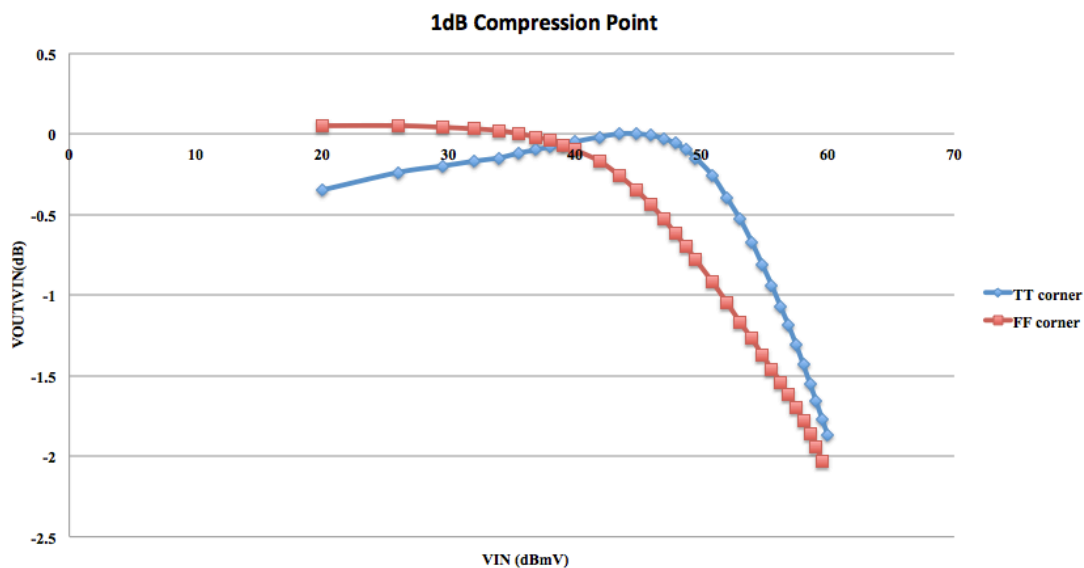


**Figure 27: 1dB Compression point at center frequency of 1GHz**

Another parameter used to measure the linearity of the circuit is the intercept point. When a single-tone signal is given as the input to a system, harmonics can be observed at multiples of the input signal frequency. As the input signal level increases, higher order harmonics also contribute to the output. Here we consider the third order and fifth order intercept points, which relate to the contribution of the third order terms and

fifth order terms to the output respectively. It has to be noted that the intercept point is a purely mathematical concept and does not refer to any physical power measurement. The intercept point is found as the point where the 3<sup>rd</sup> order or the 5<sup>th</sup> order term intercepts the fundamental frequency term.

Table 9 shows the third order and fifth order intercept points of the Roofing filter for a single tone input signal at center frequency of 1GHz and 2GHz. The third order intercept point is due to the third harmonic at three times the center frequency and fifth order intercept point is due to the fifth harmonic which occurs at five times the center frequency. In order to plot the intercept points we have run the simulations till 1V and then extrapolated the data. We have plotted the intercept points for all the three corners. From the table we can observe that the intercept points for the three corners at both frequencies are in close agreement. Generally the 3<sup>rd</sup> order and 5<sup>th</sup> order intercept points are expected to be 10-20dBmV more than the 1dB compression points. For the TT and SS corner the 3<sup>rd</sup> order and 5<sup>th</sup> order intercept points for a center frequency of 1GHz are 10dBm more than the 1dB compression points. In the FF corner the 3<sup>rd</sup> order intercept point and 5<sup>th</sup> order intercept point are 23.75dBmV and 19.46dBmV more than the 1dB compression point respectively. The higher the values of these intercept points the better is the linearity of the system.

<b>CORNER</b>	<b>IP3 POINT</b>	<b>IP5 POINT</b>
<b>TT CORNER</b>	<b>3GHz : 67.04dBmV</b>	<b>5GHz : 66.64dBmV</b>
	<b>6GHz : 68.29dBmV</b>	<b>10GHz : 69.54dBmV</b>
<b>SS CORNER</b>	<b>3GHz : 66.84dBmV</b>	<b>5GHz : 66.64dBmV</b>
	<b>6GHz : 68.29dBmV</b>	<b>10GHz : 67.23dBmV</b>
<b>FF CORNER</b>	<b>3GHz ; 67.23dBmV</b>	<b>5GHz : 66.23dBmV</b>

	<b>6GHz : 70.75dBmV</b>	<b>10GHz : 68.46dBmV</b>
--	-------------------------	--------------------------

**TABLE 9: Single tone IP3 and IP5 points for the center frequencies of 1GHz and 2GHz for all three corners**

Intermodulation is the amplitude modulation of signals that contain two or more frequencies. The intermodulation results in additional signals forming at frequencies, which are not just harmonic frequencies of the original frequency but also at sum and difference frequencies of the original frequencies and at multiples of these sum and difference frequencies. These signals are called spurious signals and often cause distortion of the original signals. In order to test how the Roofing filter we have designed is affected by the spurious signals we give two sine input signals whose frequencies are 10MHz apart. This will generate 3<sup>rd</sup> order and 5<sup>th</sup> order harmonics at frequencies  $2f_1-f_2$  and  $3f_1-2f_2$  respectively. From these frequencies we calculate the IP3 and IP5 points at all the three corners. We have calculated the intermodulation products for two sets of frequencies i.e.  $f_1 = 1\text{GHz}$  and  $f_2 = 0.99\text{GHz}$  and  $f_1 = 2\text{GHz}$  and  $f_2 = 1.99\text{GHz}$ . The first set of frequencies will generate a 3<sup>rd</sup> order harmonic at 1.01GHz and 5<sup>th</sup> order harmonic at 1.02GHz. The second set of frequencies will generate a 3<sup>rd</sup> order harmonic at 2.01GHz and 5<sup>th</sup> order harmonic at 2.02GHz.

<b>CORNER</b>	<b>IP3 POINT</b>	<b>IP5 POINT</b>
<b>TT CORNER</b>	<b>1.01GHz : 79.55dBmV</b>	<b>1.02GHz : 81.93dBmV</b>
	<b>2.01GHz : 82.27dBmV</b>	<b>2.02GHz : 83.52dBmV</b>
<b>SS CORNER</b>	<b>1.01GHz : 77.5dBmV</b>	<b>1.02GHz : 79.55dBmV</b>
	<b>2.01GHz : 74.8dBmV</b>	<b>2.02GHz : 77.5dBmV</b>
<b>FF CORNER</b>	<b>1.01GHz : 84.08dBmV</b>	<b>1.02GHz : 85.57dBmV</b>
	<b>2.01GHz : 82.92dBmV</b>	<b>2.02GHz : 84.34dBmV</b>

**TABLE 10: Double tone IMD IP3 and IP5 points**

The 3<sup>rd</sup> order intercept point and 5<sup>th</sup> order intercept points for the double tone signals are also an indicator of how well the filter can separate two closely spaced signals. The higher the value of the intercept points the better is the performance of the filter. Table 10 shows the 3<sup>rd</sup> and 5<sup>th</sup> order intercept points for the two double-tone signals. As can be seen from the results the IP3 and IP5 points are 20-30dBmV more than the 1dB compression points.

## CHAPTER 8

### EXPERIMENTAL RESULTS FOR THE ROOFING FILTER POST-LAYOUT SIMULATION

The pre-layout simulation was done in order to check the performance of the Roofing filter we designed. After obtaining satisfactory results the next step in the design process is to do the physical design or layout design of the Roofing filter. While performing pre-layout simulations we used Cadence® Spectre® as the simulation tool and the models used in the design process was from TSMC 65nm technology library. These models incorporated some of the parasitic effects that might be experienced by the devices but it cannot incorporate the parasitic effects that might occur due to the design of the layout itself. Figure 28 shows the layout of the Roofing Filter. It has to be noted that the layout has not been optimized in area. The scale in the figure represents the area of the layout to be  $342.4\mu\text{m} \times 291.3\mu\text{m}$ . After the physical design of the layout was done and it was matched with the actual schematic and a parasitic extraction was performed on the layout. The post-layout simulation helps to assess the changes in the circuit performance due to the parasitic resistances and capacitances of the layout. We try to match the results of the post-layout simulation to that of the pre-layout simulation or at least get as close as possible to it.

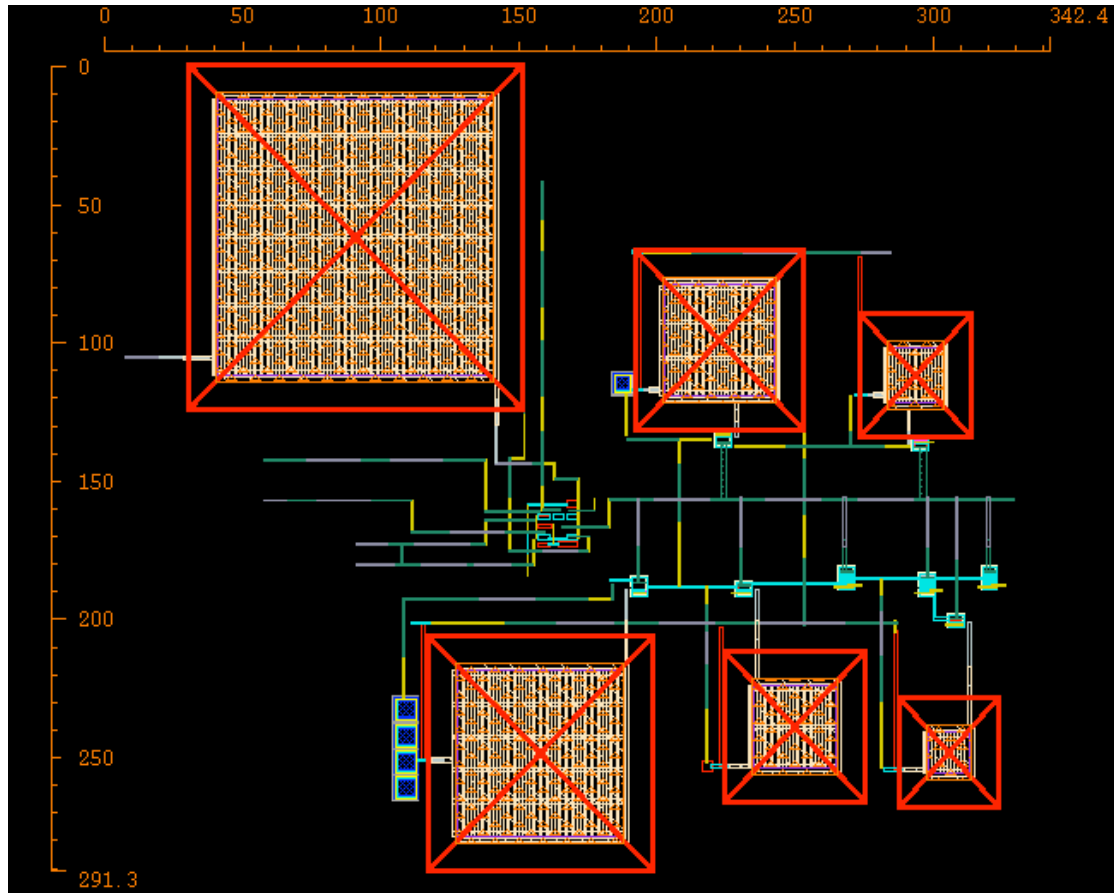


**Figure 28: Roofing Filter Layout**

### **8.1 Parasitic Extraction and Changes to the Circuit**

After the layout of the Roofing filter was designed and matched to the schematic a parasitic extraction on the layout was performed. These parasitic resistances and capacitances cause the degradation in the performance of the Roofing filter. The major factors of concern in the performance of the Roofing filter are its frequency range, insertion loss and bandwidth. The frequency range has to be from 0.7GHz to 2.7GHz. The insertion loss of the filter has to be as low as possible and we try to maintain the bandwidth of the filter to be around 200MHz. All the three performance parameters were affected due to the parasitic resistances and capacitances. After the parasitic extraction, the Roofing filter was not able to attain the range of 2GHz i.e. from 0.7GHz to 2.7GHz.

The bandwidths of the Roofing filter were very high and there was a trade-off between the range and bandwidth i.e. if the circuit was adjusted to attain the full range the bandwidth would be very high and if the circuit was designed for a low bandwidth the range could not be attained. We also tried to make adjustments to the layout but it was found that the filter was very sensitive to parasitic capacitances and resistances and much improvement could not be obtained. Hence the design of the Roofing filter had to be modified.

The first problem that had to be addressed was the frequency range of the Roofing filter. Due to the parasitic capacitances there was an increase in the effective capacitance at the output of the circuit. This increase in capacitance was preventing the Roofing filter from achieving the higher frequency ranges. The frequency range attained by the Roofing filter depends on the capacitances of the varactors. The increase in parasitic capacitances could not be compensated by reduction in the varactor capacitances. In order to overcome this problem we decided to use multiple inductors in the Roofing filter. The problem with this solution was that the inductors had to be controlled by switches to turn them on and off when required. The use of these switches would increase the series resistance of the inductor, which would in turn increase the bandwidth of the filter. Then there was also the problem of choosing the right inductor values as these inductors are off-chip and they have a fixed inductance value. The problem of inductor switching was solved by carefully selecting a low threshold voltage PMOS transistor available in the TSMC library. This transistor has a low on-resistance and hence was the apt choice. The inductors were also selected after careful experimentation. The modified Roofing filter circuit has 4 inductors with values of each inductor value being lesser than the other. The



number of inductors was set at 4 because this is the least number of inductors with which the desired frequency range and bandwidth requirements were met. The highest value inductor is directly connected to the circuit i.e. without a switch and hence it cannot be turned off. The other three inductors are connected in parallel with the help of low threshold voltage PMOS transistor switches. The other factor of concern was the bandwidth of the Roofing filter. The bandwidth increases due to the parasitic series resistance that occurs with the devices. The parasitic associated with the varactor increases with increase in varactor size. In order to reduce this we split the big varactor into varactors of smaller sizes in parallel but of the same effective capacitance.

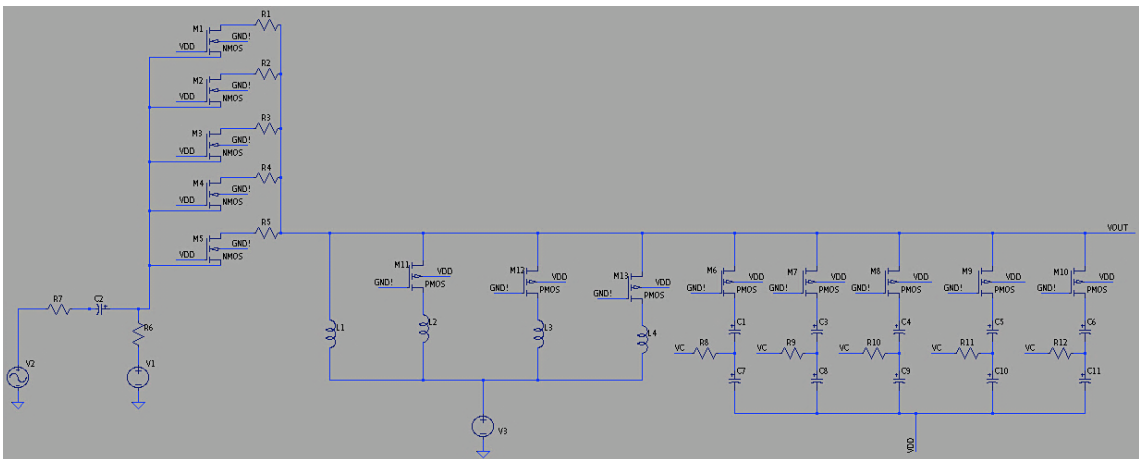


**Figure 29: Modified Roofing filter circuit**

The above figure gives the modified Roofing filter circuit that is used for post layout simulation. The following tables give the models, parameters and device sizes for all the devices used in the design of the filter.

Table 11 gives four inductor values along with their SPICE parameters that are used in the modified design of the Roofing filter. Inductor “L1” is connected to the circuit directly and the inductors “L2”, “L3” and “L4” are connected through the PMOS

transistors. These four inductors are combined in parallel and three out of these can be turned on and off to change the inductance value as required.

Inductor Model	Coilcraft 0402HP “L1”	Coilcraft 0402HP “L2”	Coilcraft 0302CS “L3”	Coilcraft 0402HP “L4”
Inductance Value	37nH	27nH	18nH	15nH
R1 Value	26 $\Omega$	30 $\Omega$	20.79 $\Omega$	15 $\Omega$
R2 Value	0.48 $\Omega$	0.275 $\Omega$	1.698 $\Omega$	0.078 $\Omega$
C Value	0.032pF	0.026pF	0.026pF	0.038pF
k	9.75E-5	6.7E-05	7.97E-06	4E-05
Rvar Value	3 $\Omega$	2.7 $\Omega$	0.356 $\Omega$	2 $\Omega$

**TABLE 11: Inductor values and SPICE parameters**

The 5 NMOS transistors and the Resistors of the resistor bank are not changed. They have the same sizes and parameters as the original schematic. Table 12 shows all the PMOS transistor sizes used in the Roofing filter circuit design. The first 5 transistors from ‘M6’ to ‘M10’ are used to control the varactor switching. The other three transistors ‘M11’ to ‘M13’ are used in inductor switching. The size of the transistors ‘M6’ to ‘M10’ has been changed to compensate for the parasitic capacitances and resistances. The transistors ‘M11’ to ‘M13’ have been sized bigger to reduce the series resistance loss of the inductors. All transistors ‘pch\_lvt’ used are low threshold voltage transistors because of their low on-resistance values. The ‘pmos\_rf’ transistors used previously have higher

parasitic and hence are replaced. The varactor sizes are also reduced, as the parasitic capacitances of the circuit have to be taken into account. The same has been done with DC block capacitors.

PMOS MODEL	TRANSISTOR SIZE	VARACTOR MODEL	VARACTOR SIZE	RESISTOR VALUE	DC BLOCK CAP VALUE
pch_lvt 'M6'	W=32um L=60nm	nmoscap_25 'C7'	W=6.8um x4 L=6.8um x4	'R8'=50K	'C1'= 7.3pF
pch_lvt 'M7'	W=24um L=60nm	nmoscap_25 'C8'	W=5.3um L=5.3um	'R9'=50K	'C3'= 3.25pF
pch_lvt 'M8'	W=16um L=60nm	nmoscap_25 'C9'	W=2.3um L=2.3um	'R10'=50K	'C4'= 1.83pF
pch_lvt 'M9'	W=8um L=60nm	nmoscap_25 'C10'	W=1.9um L=1.9um	'R11'=50K	'C5'= 0.82pF
pch_lvt 'M10'	W=6.4um L=60nm	nmoscap_25 'C11'	W=1.1um L=1.1um	'R12'=50K	'C6'= 0.463pF
pch_lvt 'M11', 'M12', 'M13'	W=64um L=60nm				

**TABLE 12: PMOS transistors sizes, varactor sizes, resistor and capacitor values**

With these new parameters the post-layout simulation is run on the Roofing filter.

## 8.2 Corner Simulations

Like in the pre-layout simulation we perform all the post-layout simulations in the three corners i.e. TT corner, SS corner and FF corner. Testing the circuit in post-layout

simulation in all the three corners is more important than doing it for pre-layout because the post-layout is the actual simulation that will decide the performance of the Roofing filter as it is closer to the real world.

### 8.2.1 Frequency Response

In order to plot the frequency response of the Roofing filter we use the same procedure as we used in the pre-layout simulation but with the exception that we also have the inductor switches that have to be controlled. The inductors are connected in parallel. At lower frequencies a high inductor value is used and this gives the required bandwidths. As the center frequency increases the inductance value needs to be decreased. Turning the inductors on adds them in parallel and hence the effective inductance reduces. Here for NMOS transistors a ‘1’ represents the transistor being on and a ‘0’ represents the transistor being off. For a PMOS a ‘1’ represents a transistor being off and a ‘0’ represents transistor being on. Once the inductor value is set we follow the same procedure as we did for the pre-layout case and set the center frequency.

CENTER FREQUENCY (GHz)	RESISTOR SWITCH SETTING	INDUCTOR SWITCH SETTING	VARACTOR SWITCH SETTING	VC (V)	VB (V)
0.7000	11111	111	00000	1.14	721.5m
0.7660	11111	111	00000	770m	743m
0.8330	11111	111	00000	400m	761m
0.9000	11111	111	01000	360m	765.5m
0.9670	11111	111	01110	350m	768m
1.0300	11111	111	10000	1.15	796m
1.1000	11100	111	10000	650m	790.5m
1.1670	11100	111	10100	750m	796m

1.2330	11000	111	10110	630m	792.5m
1.3000	11000	111	10111	450m	800m
1.3660	10000	111	11100	1.09	792m
1.4330	10000	111	11101	1.12	800m
1.5000	01000	111	11110	800m	776.5m
1.5660	10000	011	10000	600m	705.5m
1.6330	10000	011	10100	780m	715m
1.7000	10000	011	10110	800m	722.5m
1.7660	10000	011	10111	680m	733m
1.8330	10000	011	11010	860m	749.5m
1.9000	10000	011	11100	400m	759.5m
1.9660	10000	011	11101	660m	767.5m
2.0330	10000	101	11010	1.2	734m
2.1000	10000	101	11100	970m	742m
2.1660	10000	101	11101	1.11	748m
2.2330	10000	101	11110	300m	762m
2.3000	10000	001	11100	850m	733m
2.3670	10000	001	11101	1	741.5m
2.4330	10000	010	11011	400m	722m
2.5000	10000	010	11101	200m	733m
2.5660	10000	100	11011	800m	719.5m
2.6300	10000	100	11101	500m	731m
2.7000	10000	000	11101	500m	719m

**TABLE 13: Center frequencies, switch settings and Bias voltage values in TT corner**

The above table shows the switch settings of the transistors, which control the resistor bank, switch settings of the inductors and switch settings for the varactors for

each of the 31 center frequencies in the TT corner. The table also gives the bias voltages needed to set the Roofing filter to a particular center frequency.

Figure 30 shows the magnitude response of the Roofing filter in the TT corner plotted for the 31 center frequencies of interest using the data given in the table. The magnitude response is calculated for 31 frequencies in order to test the performance of the filter over the entire frequency range. It has to be noted that the filter can be adjusted to operate at any frequency in between 0.7GHz to 2.7GHz by adjusting the switch settings and the bias voltages.

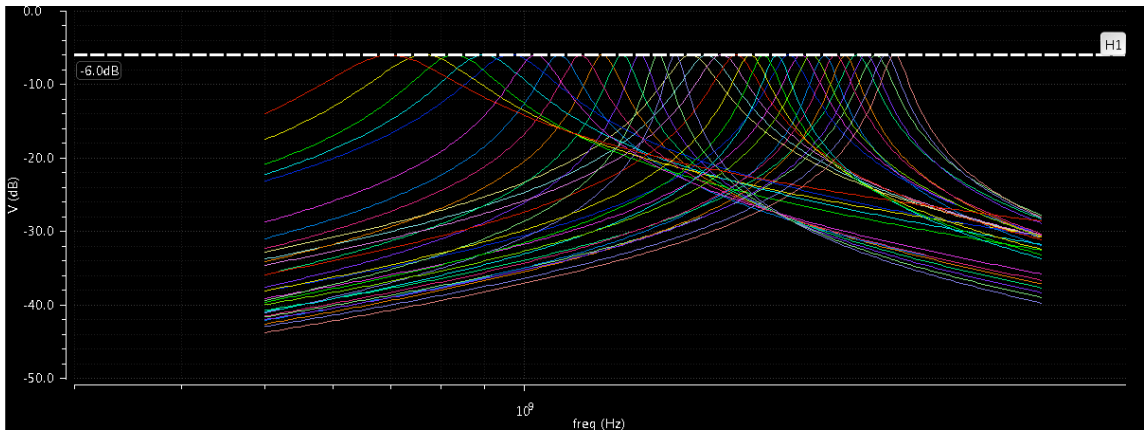


**Figure 30: Magnitude Response of the Roofing Filter in TT corner**

CENTER FREQUENCY (GHz)	RESISTOR SWITCH SETTING	INDUCTOR SWITCH SETTING	VARACTOR SWITCH SETTING	VC (V)	VB (V)
0.7000	11111	111	00000	1.2	639m
0.7660	11111	111	00000	825m	663m
0.8330	11111	111	00000	450m	684m
0.9000	11111	111	01000	430m	688m
0.9670	11111	111	01110	420m	690m
1.0300	11111	111	10000	1.18	721.5m

1.1000	11111	111	10000	700m	731m
1.1670	11111	111	10100	800m	736.5m
1.2330	11111	111	10110	700m	743m
1.3000	11111	111	10111	500m	750.5m
1.3660	11111	111	11100	1.11	754.5m
1.4330	11111	111	11101	1.15	760m
1.5000	11100	111	11110	250m	766m
1.5660	11100	011	10000	600m	676m
1.6330	11100	011	10100	800m	681.5m
1.7000	11100	011	10110	800m	688m
1.7660	11100	011	10111	700m	695m
1.8330	11100	011	11010	870m	708m
1.9000	11100	011	11100	200m	717m
1.9660	11100	011	11101	200m	718m
2.0330	11100	101	11010	1.18	694m
2.1000	11100	101	11100	950m	701m
2.1660	11100	101	11101	1.1	705m
2.2330	11100	101	11110	200m	717.5m
2.3000	11100	001	11100	700m	694.5m
2.3670	11100	001	11101	700m	703m
2.4330	11111	010	11011	300m	699m
2.5000	11111	010	11110	1.07	706.5m
2.5660	11111	100	11011	200m	699m
2.6300	11111	100	11110	1.19	703m
2.7000	11111	000	11110	200m	699m

**TABLE 14: Center frequencies, switch settings and Bias voltage values in SS corner**

Table 14 gives the switch settings and bias voltages for setting the Roofing filter to the 31 center frequencies from 0.7GHz to 2.7GHz in SS corner. Figure 31 gives the magnitude response of the filter for 31 frequencies in the SS corner.

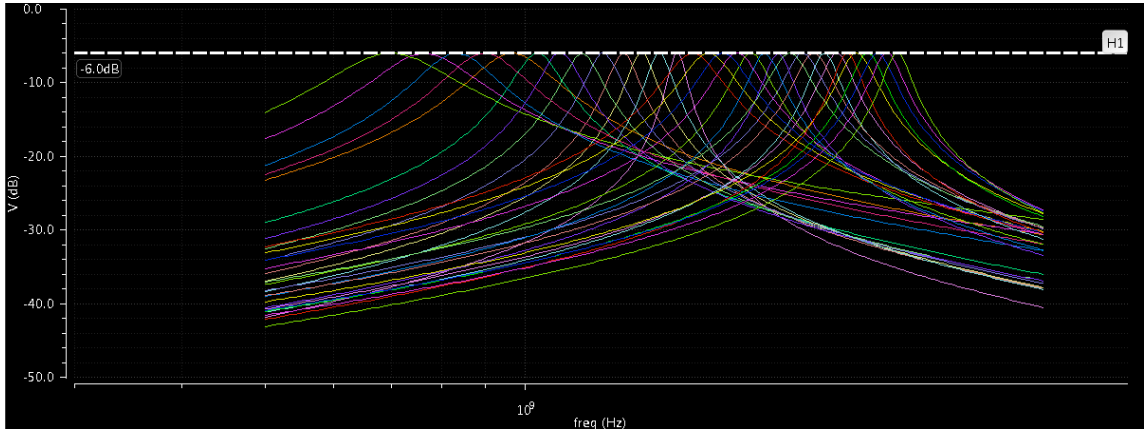


**Figure 31: Magnitude Response of the Roofing Filter in SS corner**

CENTER FREQUENCY (GHz)	RESISTOR SWITCH SETTING	INDUCTOR SWITCH SETTING	VARACTOR SWITCH SETTING	VC (V)	VB (V)
0.7000	10000	111	00000	1.09	669.5m
0.7660	10000	111	00000	730m	719m
0.8330	10000	111	00000	325m	754.5m
0.9000	10000	111	01000	290m	763.5m
0.9670	10000	111	01110	280m	769m
1.0300	01000	111	10000	1.12	795.5m
1.1000	00100	111	10000	620m	794.5m
1.1670	00100	111	10100	700m	800m
1.2330	00100	111	10110	610m	815m
1.3000	00011	111	10111	460m	815m
1.3660	00010	111	11010	200m	790m
1.4330	00010	111	11101	1.13	760m



1.5000	00010	111	11110	1	745m
1.5660	10000	011	10000	600m	770m
1.6330	10000	011	10100	750m	779.5m
1.7000	10000	011	10110	800m	785.5m
1.7660	10000	011	10111	700m	794.5m
1.8330	01000	011	11010	1	796.5m
1.9000	00100	011	11011	1.08	793m
1.9660	00100	011	11101	900m	800m
2.0330	10000	101	11001	820m	799m
2.1000	01000	101	11100	1	790m
2.1660	01000	101	11101	1.13	798m
2.2330	00100	101	11110	1.1	799m
2.3000	10000	001	11100	1	793m
2.3670	01000	001	11101	1.06	788m
2.4330	10000	010	11100	300m	787.5m
2.5000	10000	010	11101	700m	796m
2.5660	10000	100	11100	700m	785m
2.6300	10000	100	11101	900m	793m
2.7000	10000	000	11101	900m	782m

**TABLE 15: Center frequencies, switch settings and Bias voltage values in FF corner**

Table 15 gives the switch settings and bias voltages for setting the Roofing filter to the 31 center frequencies from 0.7GHz to 2.7GHz in FF corner. Figure 32 gives the magnitude response of the filter for 31 frequencies in the FF corner.

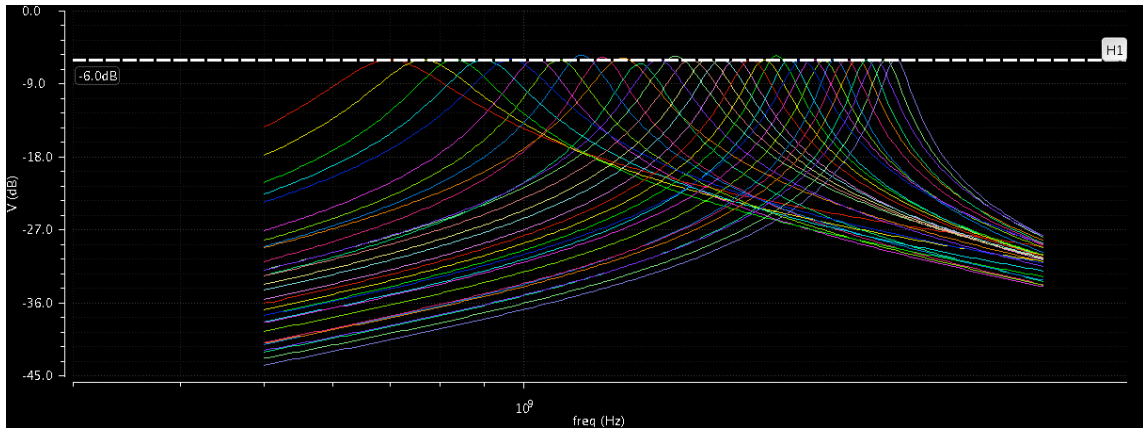


**Figure 32: Magnitude Response of the Roofing Filter in FF corner**

From this we understand that the Roofing filter we have designed is working in the post-layout and can cover the entire frequency range of 2GHz from 0.7GHz to 2.7GHz. This shows that the modifications performed to the Roofing filter in order to overcome the effects due to the parasitic resistances and capacitances worked. The filter can operate at any frequency in the range of 0.7GHz to 2.7GHz and in all the three corners as well. In order to test the performance of the Roofing filter we run further simulations in all the three corners and compare the results to that obtained for the pre-layout simulations.

### **8.2.2 Insertion loss and Bandwidth**

Insertion loss and bandwidth are the most important parameters of the Roofing filter. We had put constraints on the insertion loss and bandwidth of the Roofing filter. The insertion loss of the filter should be as low as possible so that the signal loss is minimal and the bandwidth of the filter should also be low. The lower the bandwidth the better because the Roofing filter will be used to filter out-of-band signals.

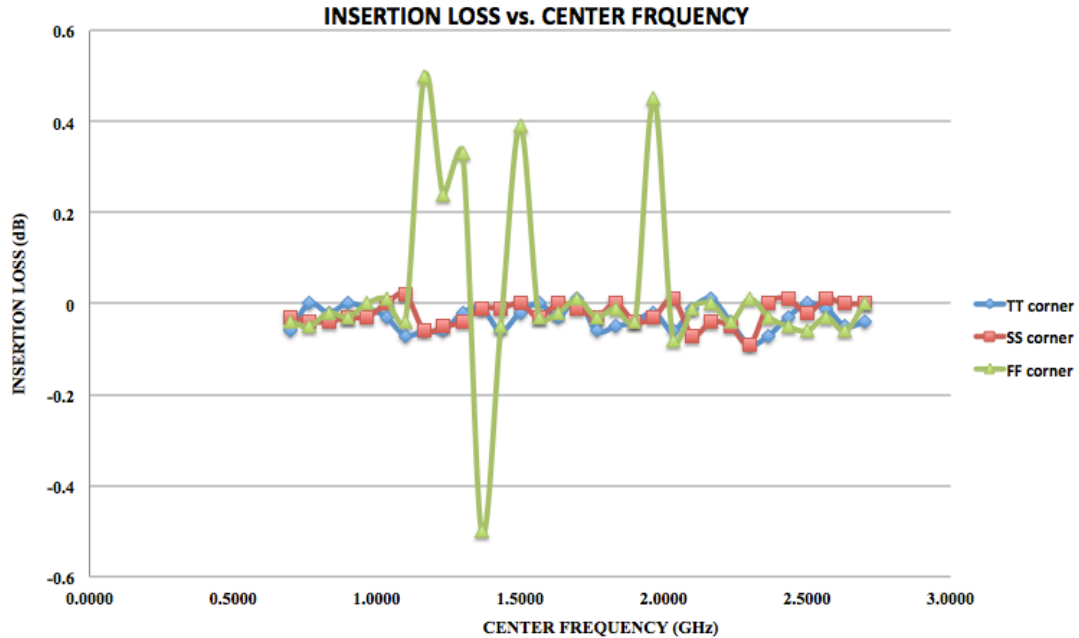


**Figure 33: Variation of Insertion loss with Center frequency for all 3 corners**

Figure 33 shows the variation of Roofing filter insertion loss with center frequency for all the three corners. As can be seen from the figure the insertion loss is very low in the TT and SS corners. The highest insertion loss in the TT corner is 0.09dB and in the SS corner it is 0.07dB. In the FF corner we observe a higher insertion loss but it is still within the accepted variation of +/- 0.5dB. The highest value of insertion loss is in the FF corner and it is 0.5dB. This shows that the loss of signal power due to the insertion loss of the filter is minimal in all the three corners.

The insertion losses obtained in the post layout simulation is almost as good as those obtained for the pre-layout simulation. Hence the effect of the parasitic capacitances and resistance on the insertion loss was reduced due to circuit modification and design.

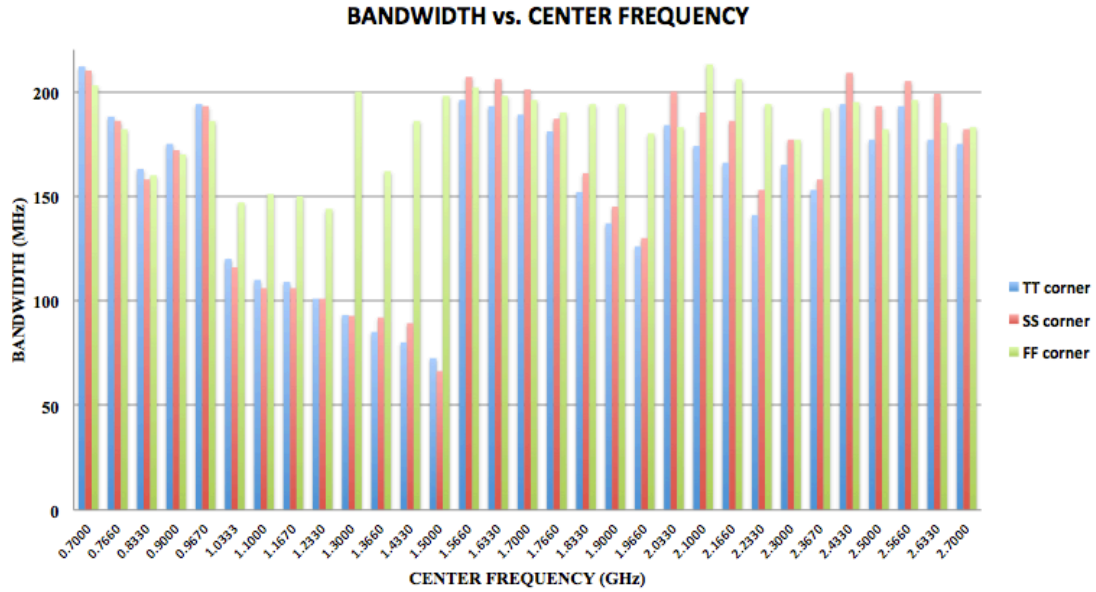


**Figure 34: Variation of Bandwidth with Center frequency for all 3 corners**

Bandwidth of the Roofing filter is another parameter that is very important. In the pre-layout simulation we tried to maintain the bandwidth around 200MHz at the highest value. This becomes increasingly difficult to maintain because of the parasitic resistances, which affect the bandwidth drastically. In order to reduce the bandwidth, the Roofing filter circuit was modified. The modified Roofing filter has 4 inductors out of which 3 are controlled by PMOS transistors to turn them on and off. The PMOS transistors have a resistance when turned on and this contributes to the increase in bandwidth. Figure 34 shows the variation of bandwidth with respect to center frequency. With the exception of a few points we have been able to maintain the bandwidth of the filter within 200MHz in all the three corners. Of those points, which are more than 200MHz, the maximum value is 213MHz. So effectively we have managed to maintain the bandwidth of the filter to be less than 213MHz throughout the entire frequency range.

The fractional bandwidth in the TT corner has a maximum value of 30.28% at center frequency of 0.7GHz. The minimum value is 4.84% at center frequency of

1.5GHz. The fractional bandwidth in the SS corner has a maximum value of 30% at 0.7GHz and a minimum value of 4.42% at 1.5GHz. In the FF corner the fractional bandwidth has a maximum value of 29% at 0.7GHz and a minimum value of 6.77% at 2.7GHz.

As can be seen from the figure there are jumps in the bandwidth between some points. These jumps occur when a varactor or an inductor is turned on, as this will create a new set of parameters for the Roofing filter and hence cause an increase in bandwidth.

Compared to the pre-layout simulation the bandwidths are little higher in the post-layout scenario. But we have restricted the highest bandwidths to be around 213MHz.

### **8.2.3 Parametric Analysis**

In the parametric analysis we vary the temperature of operation of the Roofing filter and we measure the performance of the Roofing filter. We do this for a low temperature of 0°C, nominal temperature of 27°C and a high temperature of 85°C. The parameters of the Roofing filter that are measured are bandwidth and insertion loss. This is done in all the three process corners.

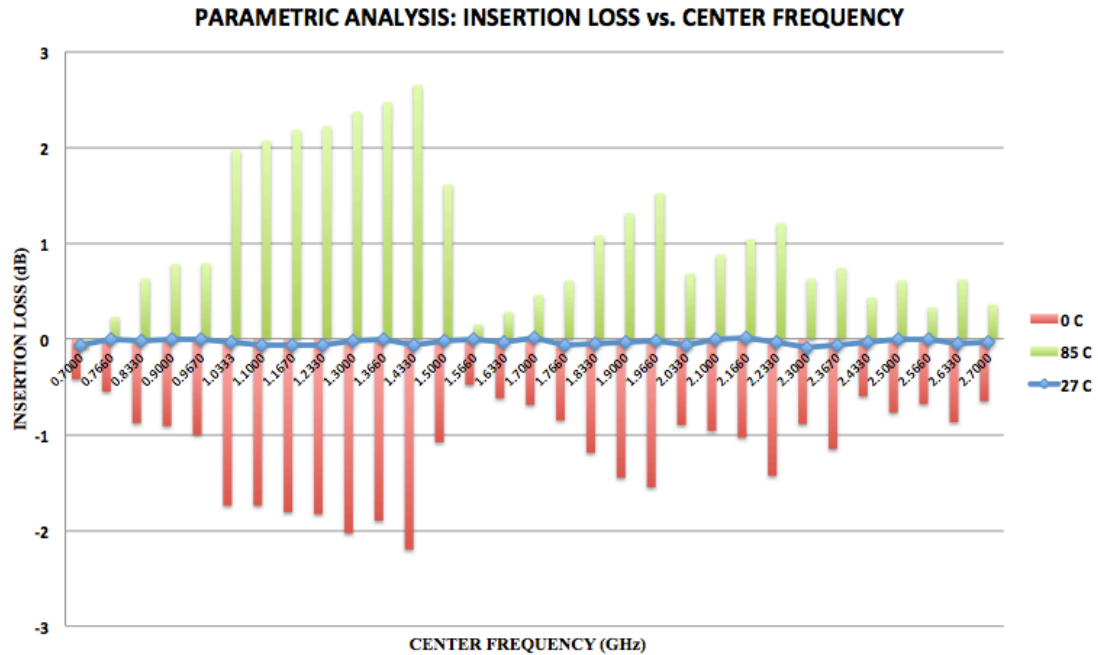


**Figure 35: Parametric Analysis: Insertion loss vs. Center Frequency in TT corner**

Figure 35 shows the variation of insertion loss with center frequency in TT corner for three temperatures. As can be seen, at room temperature the insertion loss has a very good value. We take this as reference and plot the insertion loss variation for 85°C and 0°C. As the operating temperature decreases the insertion loss increases and we also see a small shift in the center frequency to a higher value, from the ideal value. This shift in the center frequency can be attributed to the fact that the capacitance of the varactor decreases with decrease in temperature. The decrease in temperature increases the threshold voltage and increases mobility of the transistors and hence the drain currents of the transistors are increased. This increase in drain currents reduces the gain of the NMOS transistors acting as amplifiers. This is one of the reasons for the increase in insertion loss with decrease in temperature. As the temperature of operation is increased we see that the insertion loss decreases and we observe gain in the Roofing filter circuit. This is due to the fact that we have transistors at the Roofing filter input stage, which act

as a common gate amplifier and provide gain in the circuit. As the temperature increases the drain currents of these transistors decreases and hence we see more gain. There is also a small shift in the center frequency to a lower value. This can be attributed to the fact that the capacitance of varactors increases with increase in temperature.

Figure 36 shows the variation of insertion loss with center frequency for three temperature values in the SS corner. The results are similar to those obtained in the TT corner with a little enhancement at both higher and lower temperatures. This is because at the SS corner the device parameters are at their extreme values. The varactors have higher Q-factors and smaller capacitance values. As a result we observe a slightly higher variation in the center frequency as compared to the TT corner.

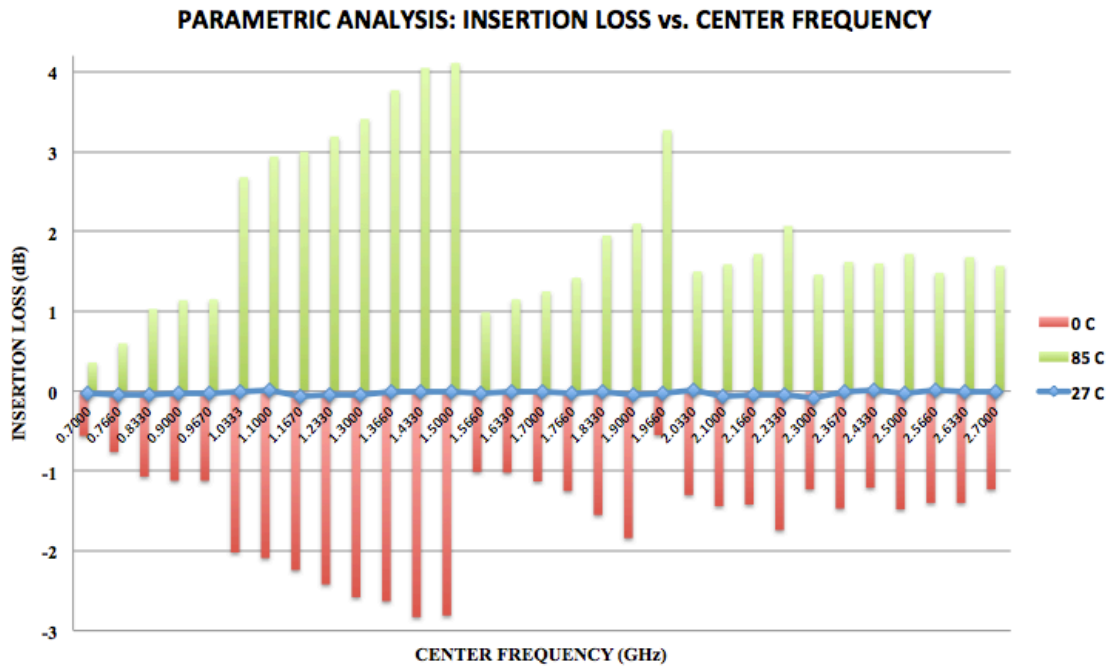
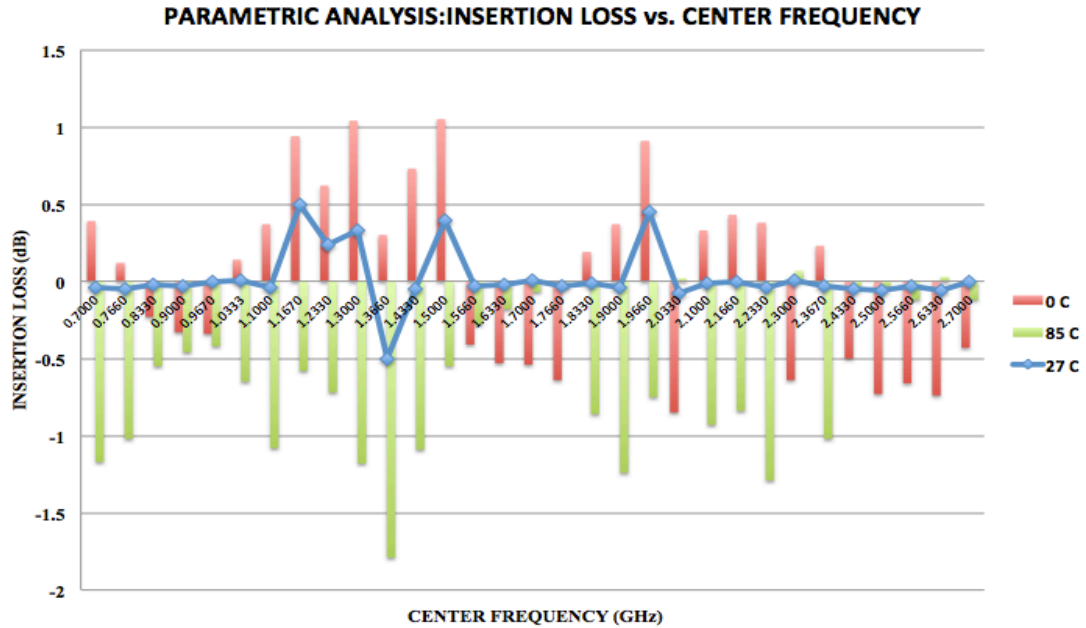


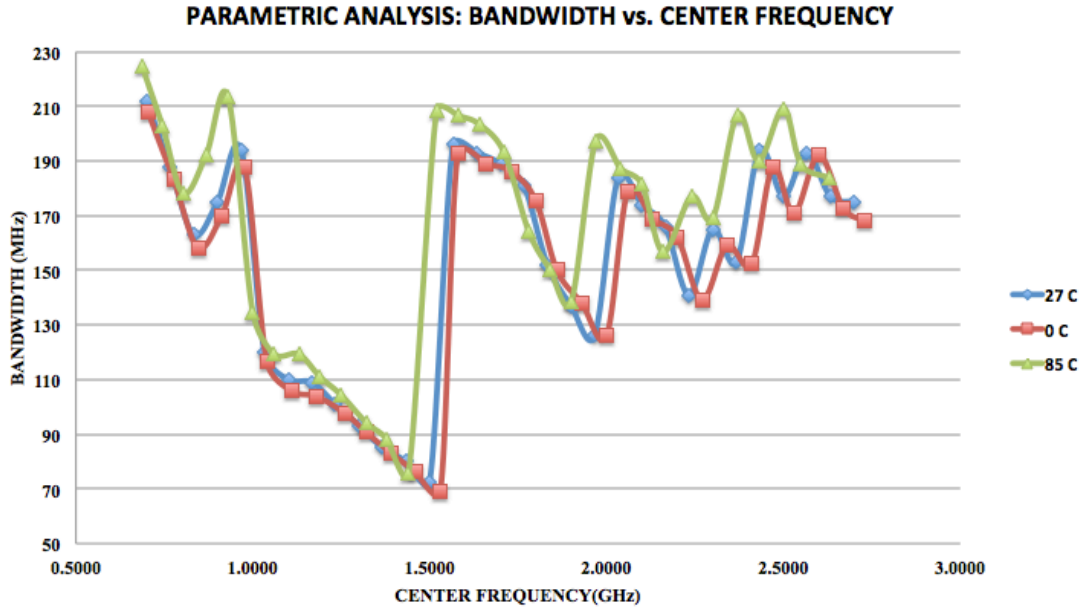
Figure 36: Parametric Analysis: Insertion loss vs. Center Frequency in SS corner



**Figure 37: Parametric Analysis: Insertion loss vs. Center Frequency in FF corner**

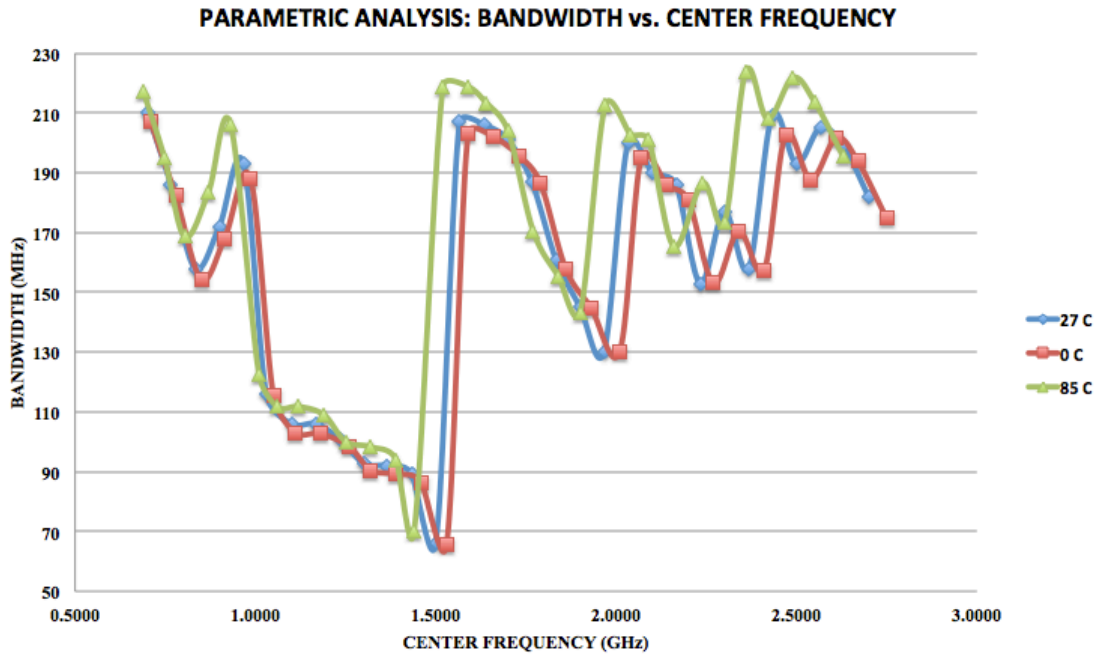
Figure 37 shows the variation of insertion with center frequency in the FF corner for three temperatures. The performance of the Roofing filter in the FF corner at the low temperature and high temperature is better than that of the TT and SS corner i.e. we see lesser variation. We also observe a change in the behavior at higher temperature i.e. we no longer see gain at higher temperature. This is due to the fact that at the FF corner the drain currents for the transistors are increased due to lower threshold voltages, shorter channel lengths etc. and hence the common gate amplifier effect is reduced to a great extent. On the other hand we see some gain in the 0°C case. This is due to the reduction in the resistance values of the resistor bank at lower temperatures.





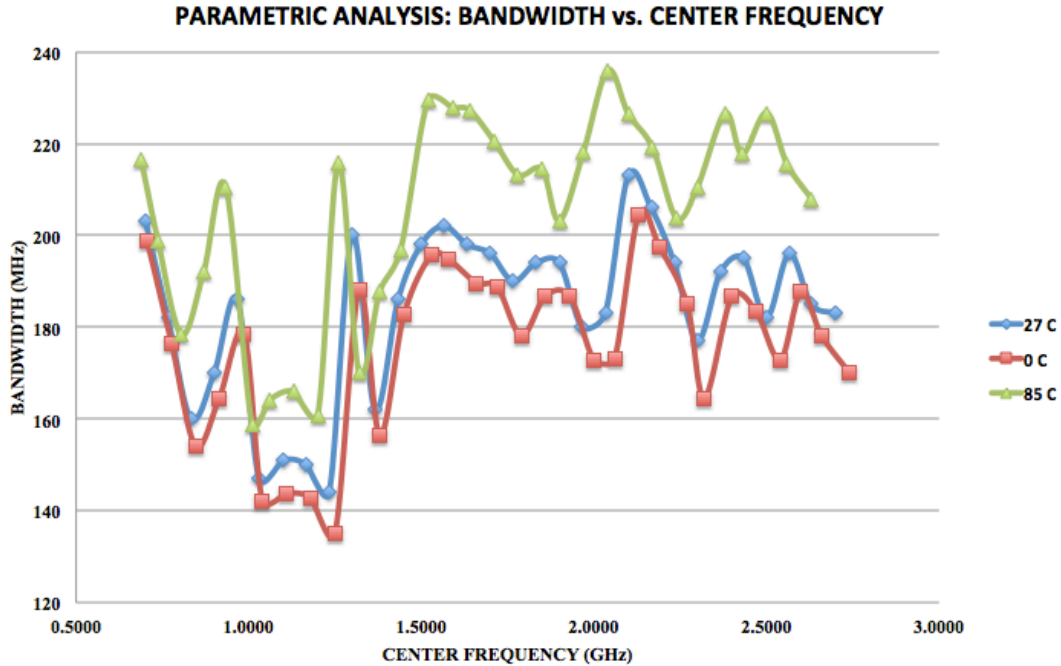
**Figure 38: Parametric Analysis: Bandwidth vs. Center Frequency in TT corner**

Figure 38 shows the variation of bandwidth with center frequency for 3 temperatures in the TT corner. As can be seen from the figure the pattern of variation is almost the same for the 3 temperature values. However we can see that the bandwidth increases with increase in temperature. The bandwidth depends on the resistance of the devices. The parasitic resistance associated with the transistors and varactors increase with increase in temperature. This results in further increase in bandwidth. But as it can be seen from the figure we have maintained the bandwidth of the Roofing filter well within 200MHz with the exception of a few points. The maximum value of the bandwidth is 225MHz which occurs at 0.7GHz center frequency at 85°C.



**Figure 39: Parametric Analysis: Bandwidth vs. Center Frequency in SS corner**

Figure 39 shows the variation of bandwidth with center frequency in the SS corner for three temperatures. Here also we observe that the pattern of variation is almost the same for all the three temperature values. The process variations in the SS corner do not have much effect on the bandwidth of the Roofing filter and hence we do not observe much deviation from the TT corner values.



**Figure 40: Parametric Analysis: Bandwidth vs. Center Frequency in FF corner**

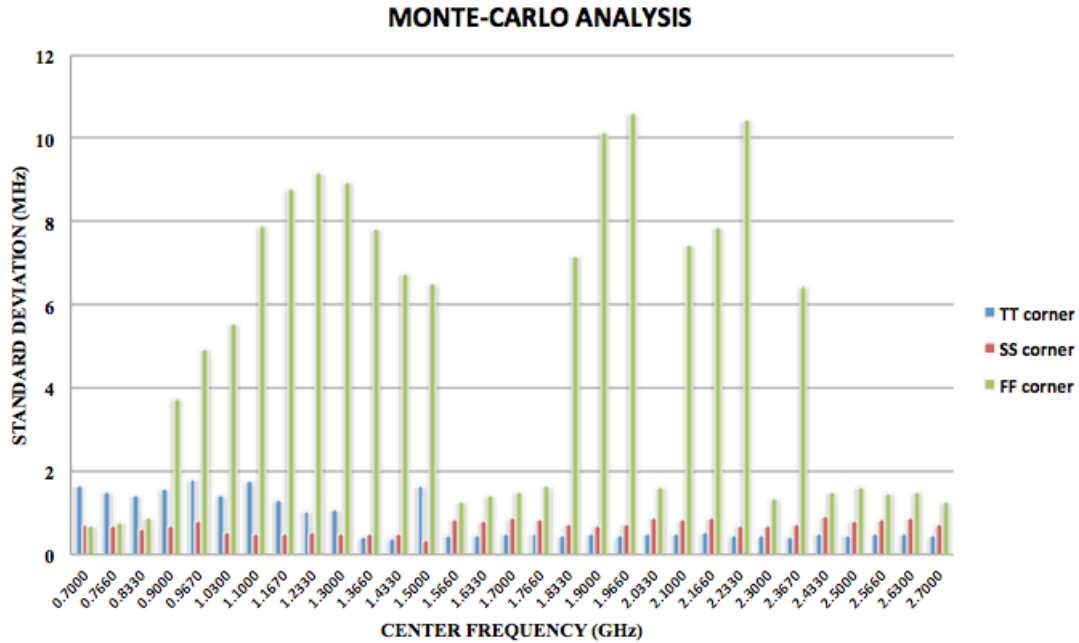
Figure 40 shows the variation of bandwidth with center frequency for three temperatures in the FF corner. In the FF corner we observe highest bandwidths among the three corners. This may be due to the fact that the varactors have low Q-factors in the FF corner. Also the parasitic resistances of the varactors and transistors increase with temperature, which contributes to increase in temperature. The maximum bandwidth observed is 235MHz at 2.1GHz center frequency and operating temperature of 85°C.

When compared to the pre-layout simulation we observe higher bandwidths in the modified post-layout circuit. This increase is due to the three extra inductors that have been added and the series resistances of the PMOS switches that control these inductors.

### 8.2.4 Monte Carlo Simulations

The statistical Monte-Carlo simulations are run to test the effect of device mismatch on the performance of the Roofing filter. As before we run the Monte-Carlo simulation in all the three corners and measure the variation in bandwidth of the filter.

Since this is a statistical simulation we run it 50 times and plot the standard deviation of bandwidth versus center frequency.



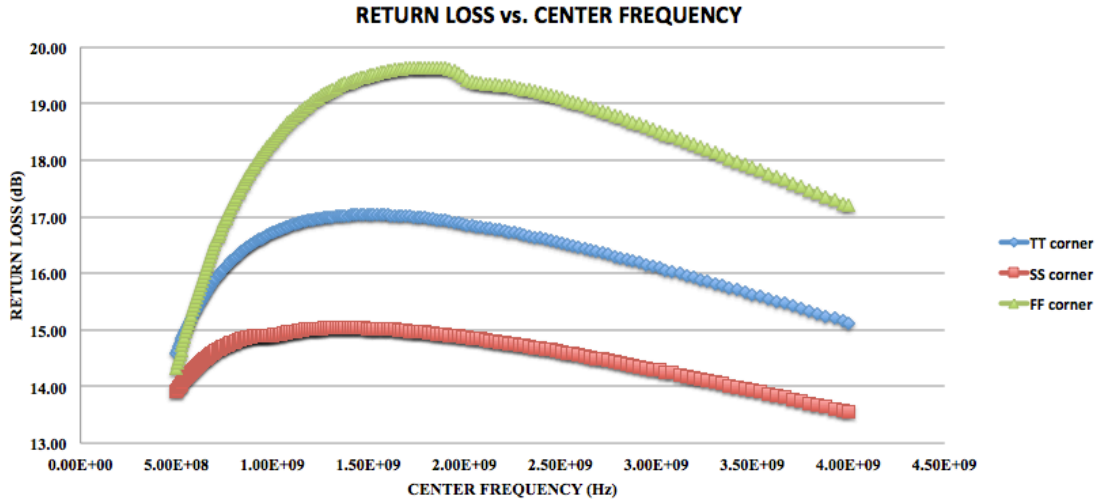
**Figure 41: Monte-Carlo Simulations for device mismatch**

Figure 41 gives this plot for all the three corners. As it can be seen from the figure the standard deviation is under 2MHz for TT and SS corner for the entire frequency range. The worst corner for the Roofing filter is the FF corner as in this corner we observe up to a maximum of 10.5 MHz of standard deviation in the FF corner at a center frequency of 2.233GHz, which has a mean bandwidth of 200.15MHz. However the worst-case bandwidth is 218MHz at 966.6MHz center frequency in the FF corner.

The performance of the Roofing filter in the Monte-Carlo simulations in the post-layout is better than that in the pre-layout. This shows that the modified Roofing filter is more robust compared to the original schematic in terms of device mismatch.

### 8.2.5 Return Loss

Return loss of the Roofing filter with respect to the change in center frequency is plotted for the three corners in figure 42. As can be seen from the figure the Return loss in the SS corner has the least value and it has the highest value in the FF corner. This means that a better source to load impedance matching is achieved in the FF corner as compared to the TT and SS corner. In the SS corner the return loss is maintained around 15dB in the frequency range of 0.7GHz to 2.7GHz. In the TT corner it varies between 16dB to 17dB in the frequency range of 0.7GHz to 2.7GHz. In the FF corner it varies from 16.5dB to 19.5dB in the frequency range of 0.7GHz to 2.7GHz.



**Figure 42: Return Loss of Roofing Filter**

### 8.2.6 Roofing Filter Linearity

Figure 43 shows the 1dB compression point analysis of the Roofing filter in all the three corners for 1GHz center frequency. In the figure we have plotted a graph of the insertion loss in dB versus input voltage in dBmV. In the TT corner we see an expansion up to 0.27dB. Taking 0.2dB as reference we get a 1dB compression point of 55dBmV. In the SS corner we see an expansion up to 0.8dB. If we take 0.5dB as reference we get the 1dB compression value as 57dBmV. In the FF corner taking 0.05dB as reference we get a

1dB compression point of 51dBmV. The higher the value of the compression points better is the linearity of the filter. This shows that our modified Roofing circuit has better performance than the original Roofing filter circuit in terms of linearity.

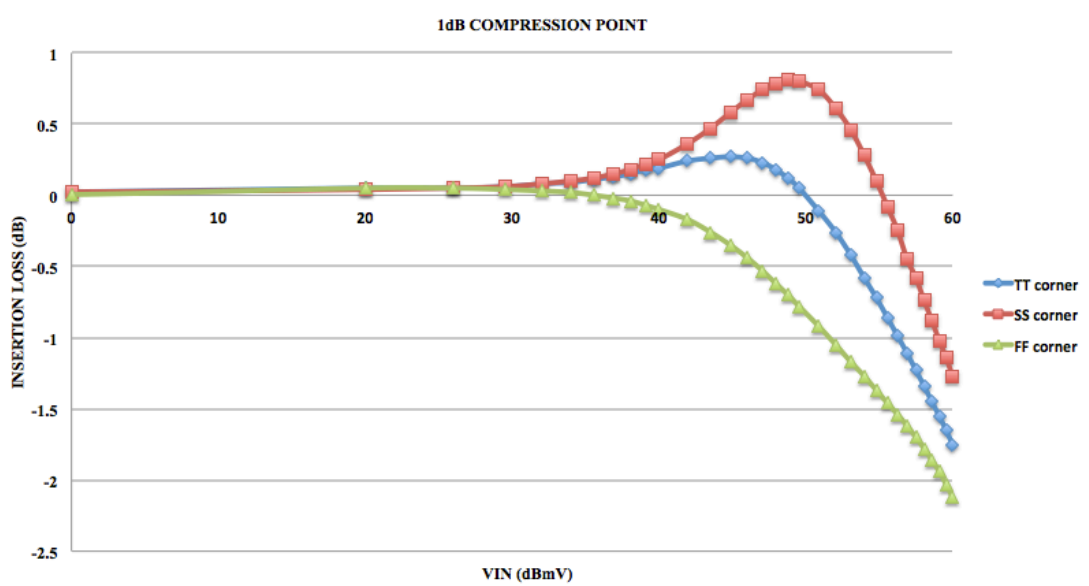


**Figure 43: 1dB compression point of Roofing Filter for 1GHz center frequency**

The 1dB compression analysis was also performed for a center frequency of 2GHz. In the TT corner and SS corner an expansion of up to 1dB was observed. If we take 1dB as the reference we get a compression point as 56.25dBmV for both the cases. In the FF corner if we take 0.2dB as reference we get a compression point of 53.06dBmV.

Another parameter used to measure the linearity is the intercept point. As before we measure the 3<sup>rd</sup> order and 5<sup>th</sup> order intercept point for a single-tone signal at two center frequencies of 1GHz and 2GHz. Table 16 gives the results obtained for these measurements. The higher the values of these intercept points the better is the performance of the filter. In the TT corner, for a center frequency of 1GHz, the 3<sup>rd</sup> order intercept point is 13.29dBmV more than the 1dB compression point and the 5<sup>th</sup> order

intercept point is 22.26dBmV more than the 1dB compression point. For a center frequency of 2GHz the 3<sup>rd</sup> order intercept point is 16.81dBmV more than the 1dB compression point and the 5<sup>th</sup> order intercept point is 17.19dBmV more. Similarly for the SS and FF corners the 3<sup>rd</sup> order and 5<sup>th</sup> order intercept points are 10-20dBmV more than the 1dB compression points.

CORNER	IP3 POINT	IP5 POINT
TT CORNER	3GHz : 68.29dBmV	5GHz : 77.26dBmV
	6GHz : 73.06dBmV	10GHz : 73.44dBmV
SS CORNER	3GHz : 66.23dBmV	5GHz : 70.62dBmV
	6GHz : 68.94dBmV	10GHz : 66.84dBmV
FF CORNER	3GHz : 68.94dBmV	5GHz : 67.42dBmV
	6GHz : 71.82dBmV	10GHz : 79.36dBmV

**TABLE 16: Single tone IP3 and IP5 points for the center frequencies of 1GHz and 2GHz for all three corners**

CORNER	IP3 POINT	IP5 POINT
TT CORNER	1.01GHz : 82.6dBmV	1.02GHz : 83.52dBmV
	2.01GHz : 82.27dBmV	2.02GHz : 83.52dBmV
SS CORNER	1.01GHz : 79.08dBmV	1.02GHz : 80.8dBmV
	2.01GHz : 79.08dBmV	2.02GHz : 80.8dBmV
FF CORNER	1.01GHz : 85.8dBmV	1.02GHz : 86.44dBmV
	2.01GHz : 87.23dBmV	2.02GHz : 88.13dBmV

**TABLE 17: Double tone IP3 and IP5 points for the center frequencies of 1GHz and 2GHz for all three corners**

Table 17 gives the 3<sup>rd</sup> order and 5<sup>th</sup> order intercept points for a double tone sine wave which are 10MHz apart around 1GHz and 2GHz center frequencies. As before we

do it for two sets of frequencies,  $f_1=1\text{GHz}$  and  $f_2=0.99\text{GHz}$  and  $f_1=2\text{GHz}$  and  $f_2=1.99\text{GHz}$ . The double tone intercept point gives us a measure of how well the filter will be able to differentiate between two closely spaced signals i.e. the higher the value of these intercept points the better. The intercept points have been calculated for all the three corners and they are 20-30dBmV more than the 1dB compression points of the corresponding center frequencies.

The performance of the modified Roofing filter is better in terms of linearity as well, compared to the original schematic and the pre-layout simulation results.

### 8.2.7 Comparison of Roofing Filter Performance with existing filters

There has been a lot of work done on the design of bandpass filters but there are no reports of a tunable narrowband filter with a wide tuning range that uses a MOSFET based varactors for center frequency tuning. Hence in order to evaluate the performance of the Roofing filter we compare it with a few different filters.

Reference	[3]	[30]	[31]	[9]	[21]	This Work
<b>Topology</b>	Dual Band Varactor based Filter	MEMS tunable BPF	65nm CMOS RF BPF	Digitally tunable BPF	Varactor Diode based BPF	65nm CMOS Passive BPF
<b>Center Frequency</b>	0.85GHz to 1.2GHz and 1.4GHz to 2.14GHz	3.4GHz to 4.2GHz	2GHz to 5GHz	450MHz to 940MHz	800MHz to 1300MHz	0.7GHz to 2.7GHz
<b>Insertion Loss</b>	0.85 to 2.42dB and 1.2 to 3.3dB	2.3dB	6dB	7.5dB	<5dB	<0.1dB
<b>Center Frequency Tuning</b>	Yes	Yes	Yes	Yes	Yes	Yes
<b>BW</b>	<156MHz and <235.4MHz		250MHz~2500MHz	>40MHz	<76MHz	<235MHz
<b>Return Loss</b>	12dB	15dB				16-17dB

**TABLE 18: Comparison of the performance of Roofing filter with existing filters**



Table 18 gives the comparison of the Roofing filter performance with a few other filters. The insertion losses obtained are far better than the other filters. The Return loss obtained is also high compared to the other filters. We tried to keep the bandwidth as low as possible. The worst-case bandwidth at the worst process corner and high temperature is around 235MHz. The circuit we have designed is also robust to process variations and device mismatches. The linearity of the filter is also good.

## CHAPTER 9

### CONCLUSIONS AND FUTURE WORK

With the advent of new standards of communication like LTE, there is a need for newer and better designs of communication systems. The first step of which was to design a filter at the receiver front end, which could operate in the entire frequency range of 0.7GHz to 2.7GHz, which is the allocated frequency range for LTE systems.

In this thesis we have presented a design for the Roofing filter, which can operate in these frequency bands and can be continuously tuned to any frequency in this range. We first designed the filter in MATLAB and verified its performance. Then we implemented the Roofing filter schematic in the TSMC 65nm CMOS technology. We ran pre-layout simulations on the circuit schematic to test its performance. This performance was kept as reference and in the post-layout simulation we tried to match the results to that of the pre-layout simulation. Parasitic resistances and capacitances affected the post-layout design and hence the original circuit was modified to obtain a better performance. All the simulations were run for the three process corners i.e. TT corner, SS corner and FF corner. This provided us with the knowledge of the circuit performance under process variations. Parametric analysis was performed to test the performance of the filter under 3 different temperatures 0°C, 27°C and 85°C. Monte-Carlo simulations were also run to test the robustness of the circuit for the worst case device mismatches in the worst process corner. Calculating the 1dB compression points, 3rd and 5th order intercept points tested the linearity of the circuit. From all these results we conclude that even though there are various areas where the design can be improved, we successfully designed a tunable integrated Roofing filter that can operate on the receiver front-end.

As a part of the future work that can be done, we can try to reduce the bandwidths of the Roofing filter further. The LTE have channels as small as 1.4MHz to 20MHz. Hence lesser the bandwidth the better is the performance of the filter.

There are 13 transistor switches, which control the resistors, inductors and varactors. These switches are now being set manually. But in an actual circuit we would like to use DACs to control these switches. We would also want the other control voltages to be supplied through an on-chip circuit. We could use an SPI bus for this purpose.

We can also reduce the number of varactors used by placing two varactors back to back. This will require 3 varactor control voltages instead of one but the tuning range achieved will be better.

## BIBLIOGRAPHY

- [1] Ahmed, H., Devries, C. and Mason, R., "RF, Q-enhanced bandpass filters in standard 0.18 $\mu$ m CMOS with direct digital tuning," Proc. ISCAS '03, May 2003, pp. I-577 – I-580.
- [2] A. R. Brown and G. M. Rebeiz, "A Varactor-Tuned RF Filter," Proc. IEEE Trans. On Microwave Theory and Techniques, Vol. 48, Jul. 2000, pp. 1157-1160.
- [3] Chaudhary, G., Yongchae, J. and Jongsik, L, "Harmonic Suppressed Dual-Band Bandpass Filters with Tunable Passbands," IEEE Trans. On Microwave Theory and Techniques, Vol. 60, Jul. 2012, pp. 2115-2123.
- [4] Chung-Yu, Wu and Shuo-Yuan, Hsiao, "The Design of a 3-V 900-MHz CMOS bandpass amplifier," IEEE Journal of Solid-State Circuits, Vol. 32, Feb 1997, pp. 159-168.
- [5] Doberstein, S., "Switchable Low-Loss SAW Filter Banks with MEMS Switches," Proc. IEEE IUS, Oct. 2010, pp. 1294-1297.
- [6] Elhallabi, H., Fouzar, Y. and Sawan, M. "High frequency CMOS Gm-c bandpass filter with automatic on-chip tuning," ICECS, 2001, Vol. 2, pp. 823-826.
- [7] Hunter, I.C. and Rhodes, J.D., "Electronically Tunable Microwave Bandpass Filter," Proc. IEEE Trans. On Microwave Theory and Techniques, Vol. 30, Sep. 1982, pp. 1354-1360.
- [8] Howes, M.J. and Morgan, D.V., " Variable Impedance Devices," Ch.1, New York: Wiley, 1978
- [9] Jaschke, A. et al., "Digitally tunable bandpass filter for cognitive radio applications," IEEE workshop on CAMAD, Sept. 2012, pp. 338-342.

- [10] Kuhn, W.B, Nobbe, D., Kelly, D. and Orsborn, A.W., "Dynamic range performance of on-chip RF bandpass filters," IEEE Trans. On Circuits and Systems II: Analog and Digital Signal Processing, Vol. 50, Oct. 2003, pp. 685-694.
- [11] Lee, C.-H., Cornish, J., McClellan, K. and Choma, J., Jr., "Current-mode approach for wide-gain bandwidth product architecture," IEEE Trans. On Circuits and Systems II: Analog and Digital Signal Processing, Vol. 45, May. 1998, pp. 626-631.
- [12] Loy, Matt, "Understanding and Enhancing Sensitivity in Receivers for Wireless Applications," Texas Instruments, Tech. Brief, May 1999.
- [13] McKinley, S. and Levine, M., "Cubic Spline Interpolation,"  
<http://online.redwoods.cc.ca.us/instruct/darnold/laproj/fall98/skymeg/proj.pdf>
- [14] Naderi, A., Sawan, M. and Savaria, Y., "A 1-mw 2-GHz Q-enhanced LC bandpass filter for low-power RF applications," Proc. IEEE-NEWCAS Conference, 2005, pp. 365-368.
- [15] Nguyen, N.M. and Meyer, R.G., "Si IC-compatible inductors and LC passive filters," IEEE Journal of Solid-State Circuits, Vol. 25, Aug. 1990, pp. 1028-1031.
- [16] Niknejad, A.M. and Meyer, R.G., "Analysis of eddy-current losses over conductive substrates with application to monolithic inductors and transformers," IEEE Trans. on Microwave Theory and Techniques, Vol. 49, Jan. 2001, pp. 166-176.
- [17] Nogorodov, V., Freisleben, S., Hornsteiner, J., Schmachtl, M., Vorotnikov, B., Heide, P., Vossiek, M., "Compact low-loss 2.4GHz ISM-band SAW bandpass filter on LTCC substrate," Proc. APMC, Dec. 2009, pp. 2072-2075.

- [18] Oualkadi, A.E., El Kaamouchi, M., Paillot, J.-M., Vanhoenacker-Janvier, D., Flandre, D. "Fully Integrated High-Q Switched Capacitor Bandpass Filter with Center Frequency and Bandwidth Tuning," Proc. IEEE RFIC Symposium, June 2007, pp. 681-684.
- [19] Pipilos, S. and Tsividis, Y., "Design of active RLC integrated filters with applications in the GHz range," IEEE ISCAS, 1994, Vol. 5, pp. 645-648.
- [20] Pozar, D., "Microwave Engineering", Third edition, Chapter 8
- [21] Reck, C., Trommer, R. and Schmidt, L-P., "Bandpass filter with tunable bandwidth and center frequency based on varactor diodes", German Microwave Conference, March 2011, pp.1-4
- [22] Suárez, M., Villegas, M., Baudoin, G., "RF and microwave band-pass passive filters for mobile transceivers with a focus on BAW technology," Université Paris-Est, Laboratoire ESYCOM, Groupe ESIEE Paris, France, pp.152-174
- [23] Soorapanth, T., "CMOS RF FILTERING AT GHZ FREQUENCY," Dissertation, Stanford University, Aug. 2002.
- [24] Trzcinski, T., "Surface Acoustic Wave (SAW) filter technology," Project, Torino, 2008
- [25] Voghell, J.-C. and Sawan, M., "Current tunable CMOS transconductor for filtering applications," Proc. ISCAS, 2000, Vol. 5, pp. 165-168.
- [26] Winder, Steve, "Analog and Digital Filter Design," USA: Elsevier Science, 2002.
- [27] Worawat Sa-ngiamvibool, "Existing Techniques for Bandpass Filters- An Overview," [http://www.resjournal.kku.ac.th/article/15\\_07\\_592.pdf](http://www.resjournal.kku.ac.th/article/15_07_592.pdf), Mahasarakham University, Thailand, Jul. 2010, pp. 592-609.
- [28] "SPICE Model-0302CS," Datasheet, Coilcraft, Inc., 2009, Doc. 158.
- [29] "Chip Inductors-0302CS Series (0805)," Datasheet, Coilcraft, Inc., 2010, Doc. 302-1.

- [30] Xiaoyu Mi, Toyoda, O., Ueda, S. and Nakazawa, F., "Miniaturized microwave tunable bandpass filters on high-k LTCC with integrated resistive vias as bias-T," Proc. IEEE Microwave Symposium Digest, June 2011, pp. 1-4.
- [31] Yixiao Wang, Le Ye, Huailin Liao and Ru Huang, "Cost-efficient CMOS RF tunable bandpass filter with active inductor-less biquads," IEEE ISCAS, May 2012, pp. 2139-2142.
- [32] Zhiqun Li et al., "Accumulation-mode MOS varactor modeling for RF applications valid up to 40GHz," ICMMT, 2010, pp. 885-888.
- [33] <<http://www.tsmc.com/english/dedicatedFoundry/technology/65nm.htm>>
- [34] <http://www.4gamericas.org>
- [35] "SPICE Model-0402HP," Datasheet, Coilcraft, Inc., 2009, Doc. 158-23.
- [36] "Chip Inductors-0402HP Series (1005)," Datasheet, Coilcraft, Inc., 2010, Doc. 526.